X-ray Scattering During Shear and Processing of Polymers

Wesley Burghardt
Department of Chemical & Biological Engineering
Northwestern University

Outline

- Motivation
- Scattering fundamentals
- X-ray scattering in shear
  - Characterization of orientation
  - Experimental aspects
  - Case studies
    - Liquid crystalline polymers
    - Block copolymers
    - Nanocomposites
- Processing
- Extensional Flow

Motivation:
Polymer structure under flow

- As a rheologist…
  - Seek to understand microscopic origins of non-Newtonian flow behavior
- As a physicist…
  - Structural response to applied fields opens window into molecular/microstructural dynamics
- As a materials scientist…
  - Organization of materials by applied flow can facilitate characterization, produce anisotropic microstructures
- As an engineer…
  - Impact of processing on final product properties

Possible approaches

- Microscopy: Real-space imaging
  - Typically only optical microscopy applied to flow
  - Examples: DNA visualization; colloidal dispersions
- Polarimetry: ‘Rheo-optics’
  - Flow birefringence, dichroism
- Scattering: Reciprocal space
  - Light, neutron & x-ray scattering have all been applied to study structure of complex fluids during shear
  - Essential phenomena:
    - Interaction of incident radiation with sample
    - Constructive/destructive interference of radiation scattered from different locations within material

Interference: double slit expt

- Recall from physics

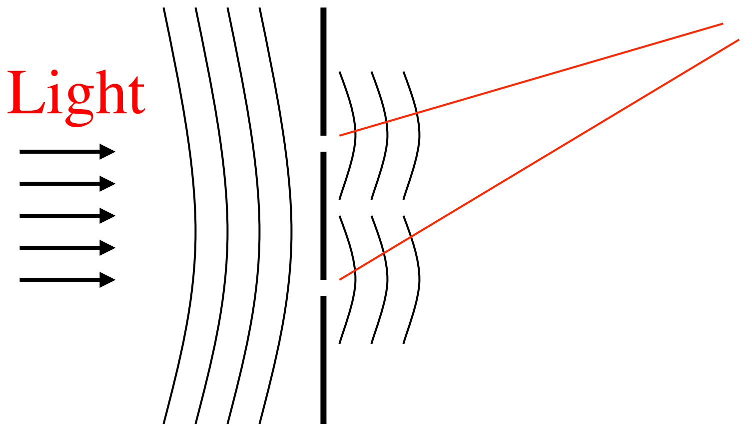

• different path lengths from light arriving from different slits
• phase difference
• constructive/destructive interference
• fringe pattern

For successive bright fringes,

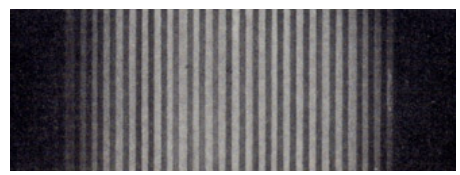

$$\sin\theta = \frac{m\lambda}{d}$$

- Comments
  - Observation of interference pattern allows one to determine slit spacing
  - Smaller spacing of slits --> larger angles needed to accumulate significant phase difference & interference

Scattering & interference

- Scattering geometry

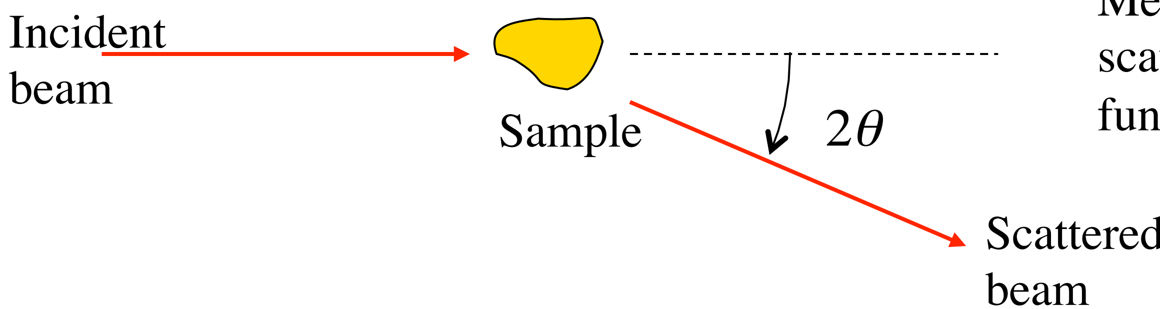

Measure intensity of scattered radiation as function of scattering angle

- Interference calculation: Two points *O* & *P*

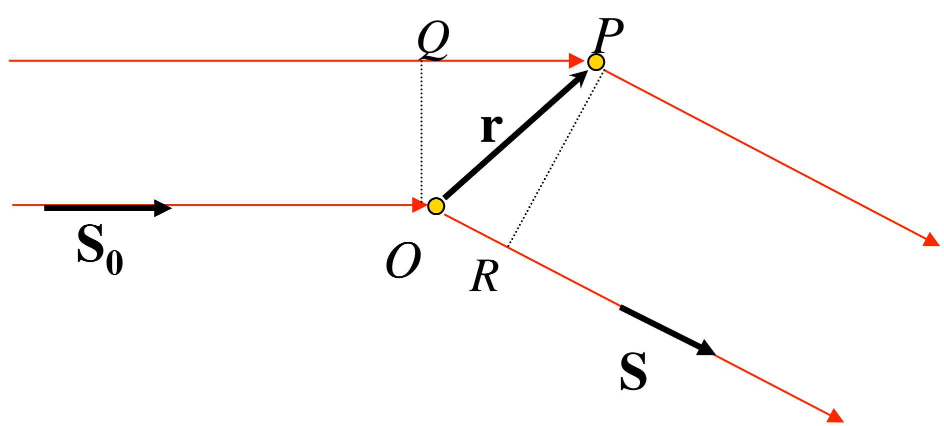

$$\text{Path dif.} = \overline{QP} - \overline{OR}$$

$$= \mathbf{S}_0 \cdot \mathbf{r} - \mathbf{S} \cdot \mathbf{r}$$

$$\text{Phase dif.} = \frac{2\pi}{\lambda}(\mathbf{S}_0 \cdot \mathbf{r} - \mathbf{S} \cdot \mathbf{r})$$

$$= -\frac{2\pi}{\lambda}(\mathbf{S} - \mathbf{S}_0) \cdot \mathbf{r}$$

$$= -\mathbf{q} \cdot \mathbf{r}$$

Scattering vector

Scattered amplitude

- Add up scattering contributions from each part of sample
- Allow for interference using phase factor computed above

$$A(\mathbf{q}) = \int_V \rho(\mathbf{r}) e^{-i\mathbf{q}\cdot\mathbf{r}} d\mathbf{r} \qquad I(\mathbf{q}) = \left|A(\mathbf{q})\right|^2$$

Distribution of 'scattering power' (e.g. electron density for x-rays)

Phase factor

- 3-D Fourier transform
- Maps 3-D real-space structure into 3-D 'reciprocal' space

Scattering vector & reciprocal space

$$\mathbf{q} = \frac{2\pi}{\lambda}(\mathbf{S} - \mathbf{S_0})$$

$$q = |\mathbf{q}| = \frac{4\pi}{\lambda}\sin\theta$$

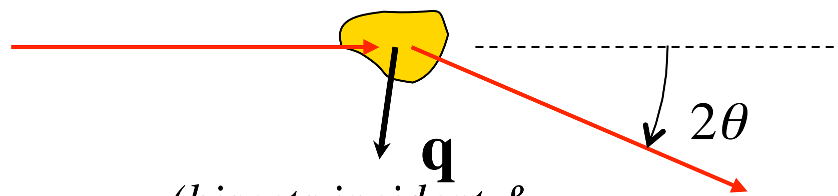

(bisects incident & scattered beam directions)

As scattering angle varies over all possible directions, tip of **q** defines a spherical surface ('Ewald sphere'). Hard to fully characterize $I(\mathbf{q})$!

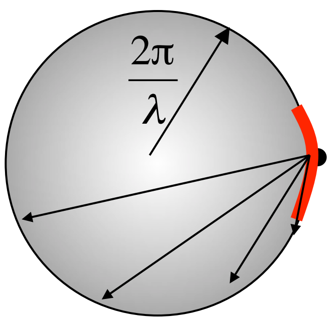

Special case: small-angle scattering

Here, **q** 'lives' roughly in the plane perpendicular to incident beam direction. Experiments sample a 'slice' of reciprocal space.

Length scales & scattering

$$A(\mathbf{q}) = \int_V \rho(\mathbf{r}) e^{-i\mathbf{q}\cdot\mathbf{r}} d\mathbf{r}$$

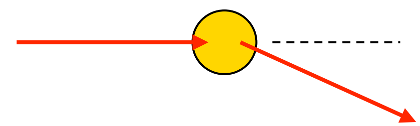

- Consider scattering from sphere
  - If $R << 1/q$, then significant phase differences do not accumulate; no destructive interference
  - Require qR ~ O(1) to see significant destructive interference & associated drop in scattered amplitude & intensity
  - As R increases, interference sets in at progressively smaller values of q
  - Small-angle scattering ⟶ larger structures

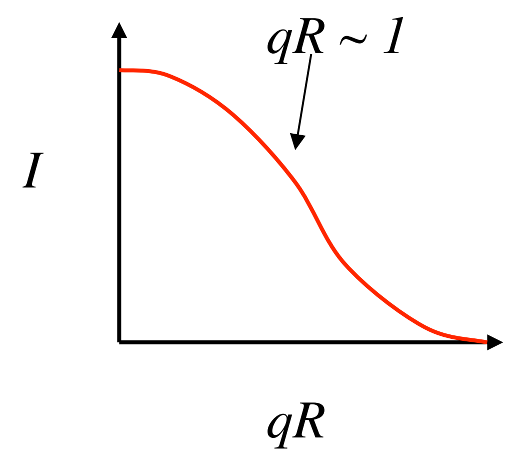

Anisotropic shapes & interference

- Flow-induced structures are generally anisotropic

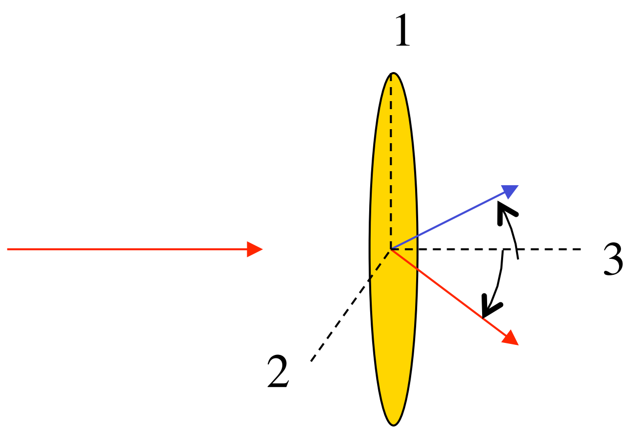

If scattered beam lies in 2-3 plane, object seems small; little interference until large angle (q)

If scattered beam lies in 1-3 plane, object seems big; opportunity for interference at smaller q

- Amplitude/intensity distribution in reciprocal space:

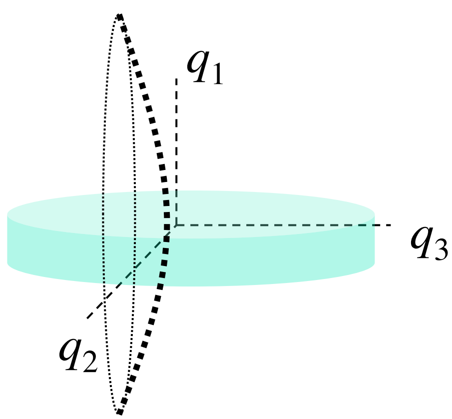

But, in a typical scattering experiment we only see that slice of reciprocal space defined by Ewald sphere.

Schematic 2D scattering patterns

Real space | Reciprocal space | Pattern

Rods

Disks

Periodic layers

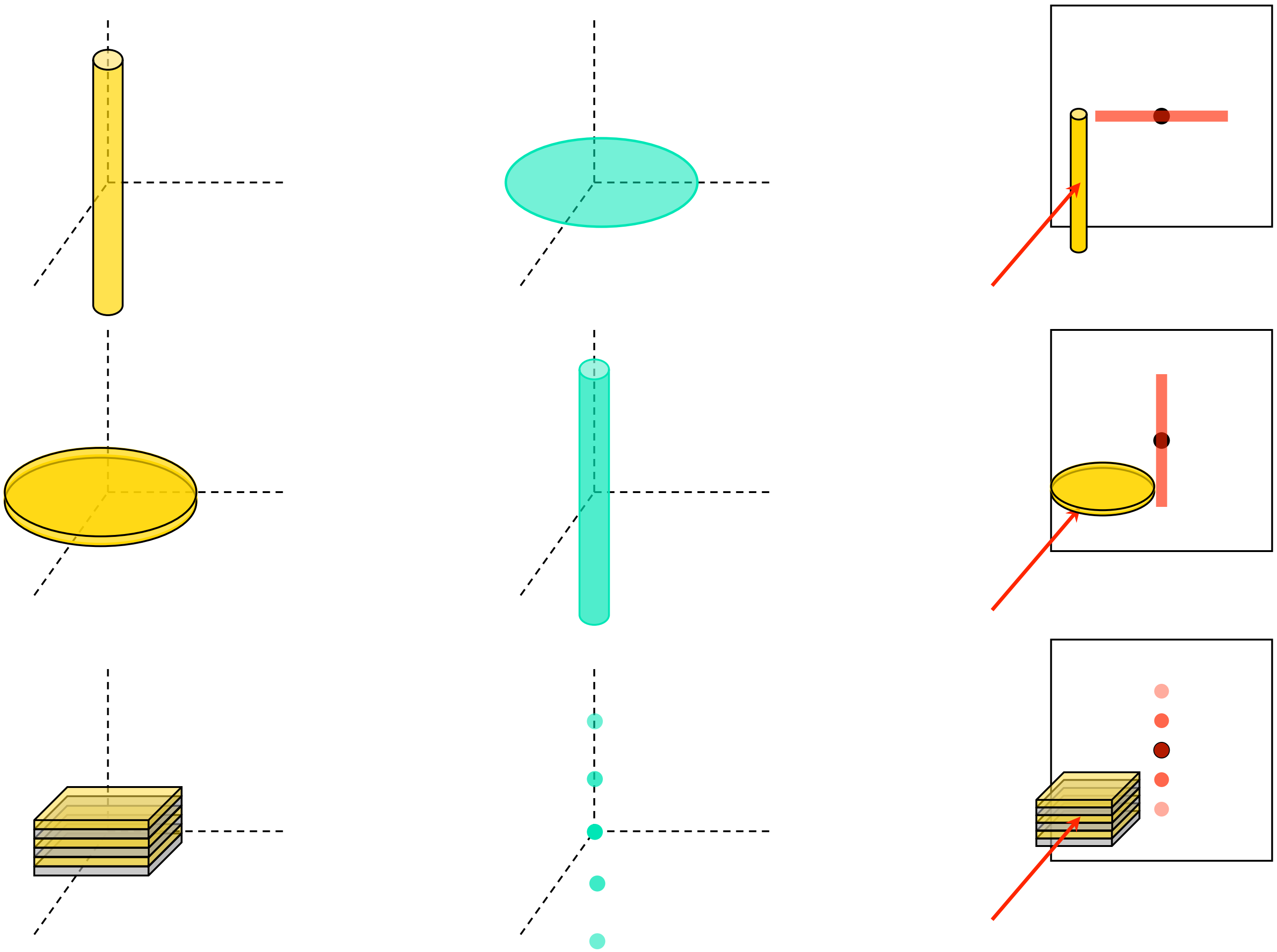

Probing reciprocal space: *In situ* scattering in shear flow

2-direction: 1-3 plane

3-direction: 1-2 plane

1-direction: 2-3 plane

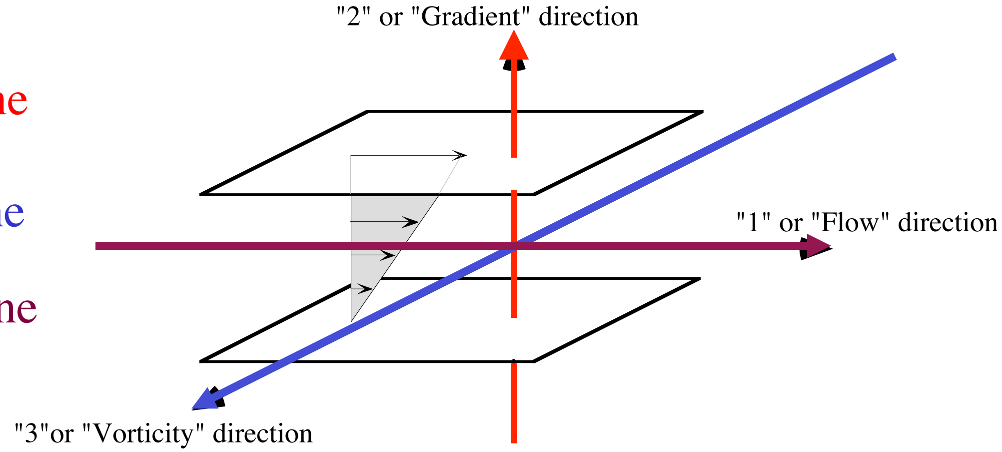

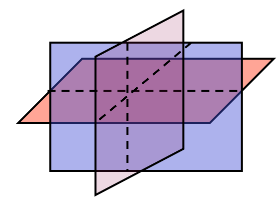

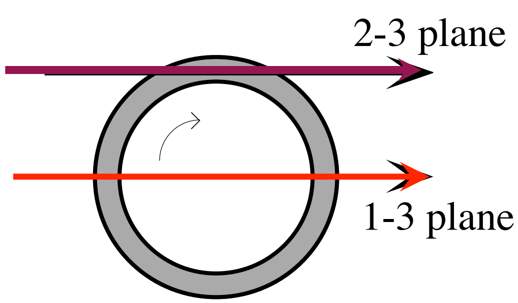

Couette

Neutron & x-ray

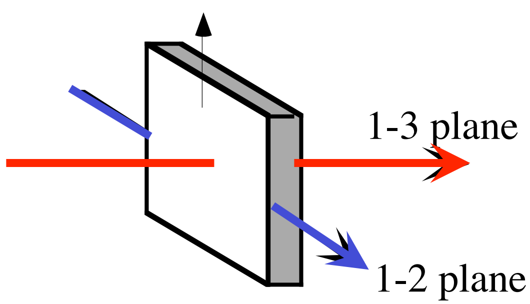

Linear shear

Neutron, x-ray

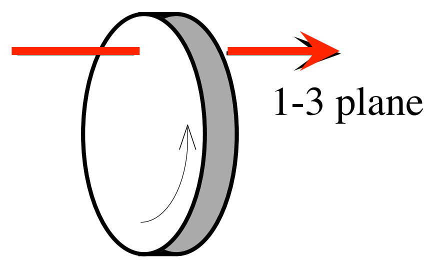

Rotating disk

X-ray, light

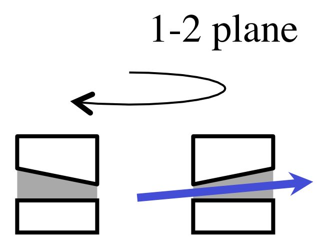

Annular C&P

X-ray

Representation and quantification of orientation state

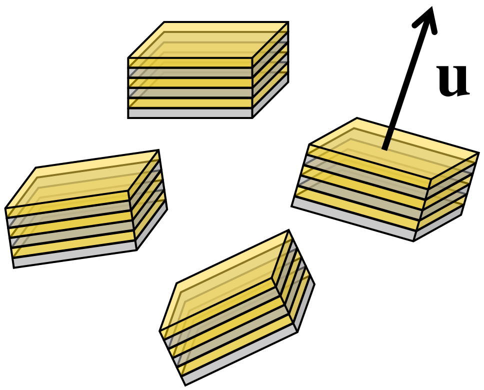

Orientation probability distribution function, $\psi(\mathbf{u})$

$\mathbf{u}$ 'lives' on unit sphere: $\psi(\beta,\phi)$

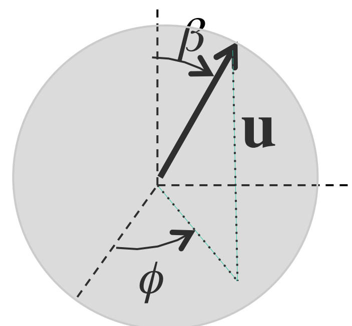

For *uniaxial* distribution of orientation, $\psi = \psi(\beta)$

For anisotropic distribution of 1-D layered objects, distribution of diffracted intensity in reciprocal space directly reflects $\psi(\mathbf{u})$.

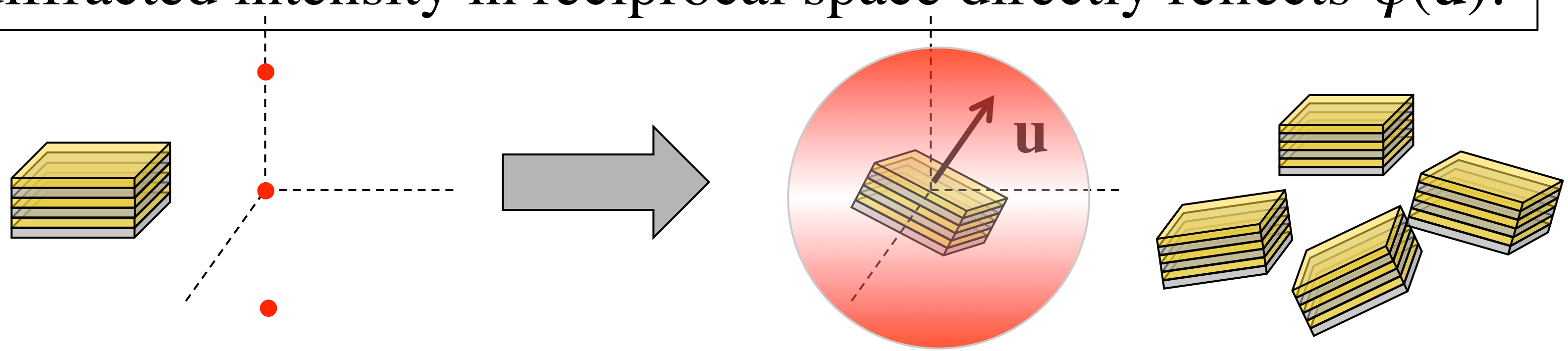

Uniaxial orientation distribution: 'Order parameter'

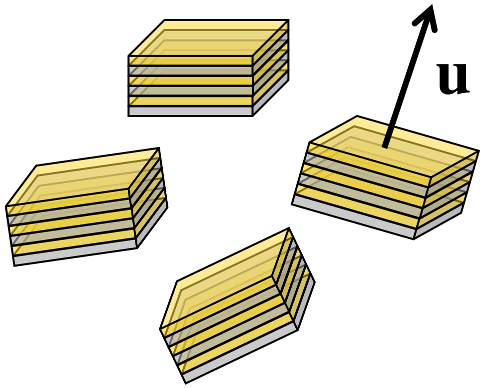

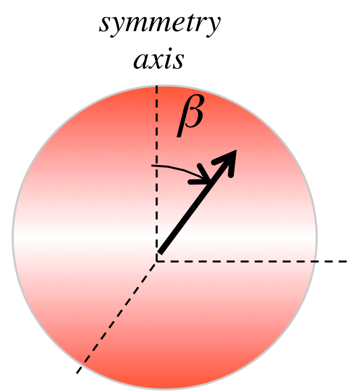

$$\langle \cos^2 \beta \rangle = \int_0^{\pi/2} \cos^2 \beta \, \boxed{\psi(\beta)} \sin \beta \, d\beta$$

$$S = \frac{3\langle \cos^2 \beta \rangle - 1}{2}$$

$S = 1$ for perfect orientation
$S = 0$ for random orientation

Idealized 2-D scattering experiment:

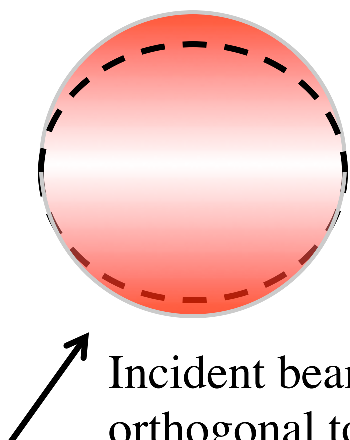

Incident beam orthogonal to symmetry axis

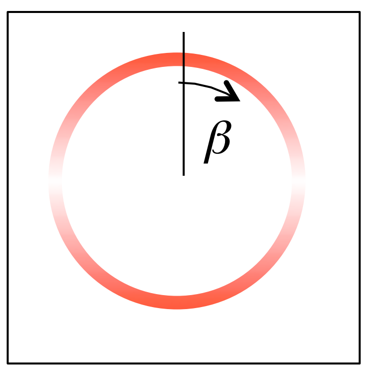

2-D pattern

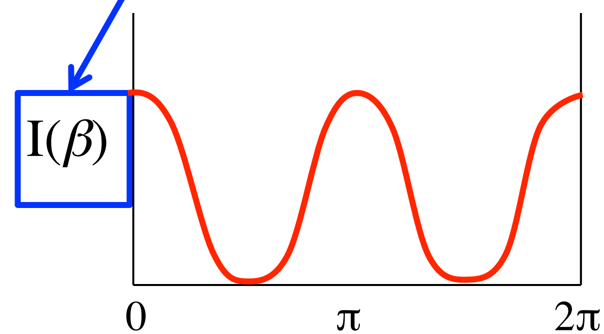

Azimuthal scan

Fine Print #1

- Due to curvature of Ewald sphere, never realize a true 2-D 'slice' of reciprocal space; cannot 'see' $\beta = 0$ in this type of geometry:

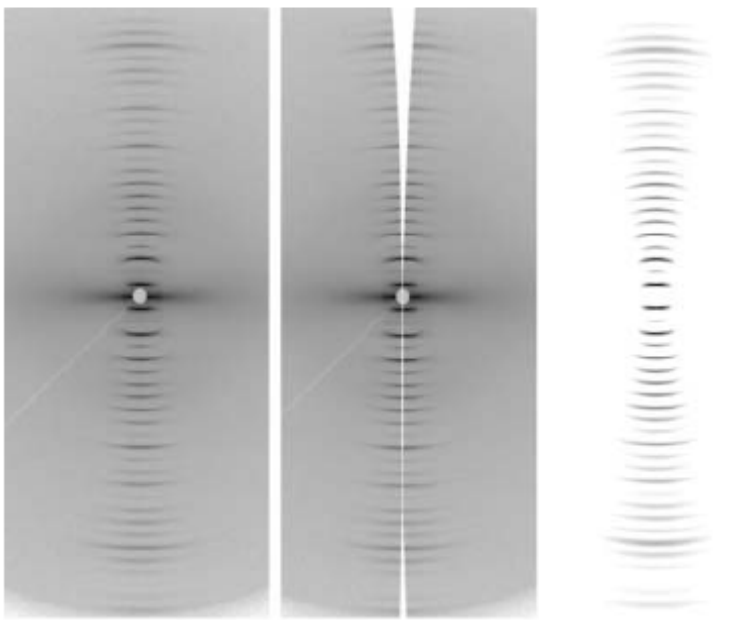

(a) As measured. (b) Corrected. (c) Calculated.

Burger, Hsiao & Chu, *Polymer Reviews*, **50**, 91 (2010)

SAXS: not a big deal, unless highly oriented

WAXS: bigger concern

One solution: progressively tilt sample; bring symmetry axis 'into view' (not practical for shear studies)

Fine print #2

- Shear flow generally does NOT produce uniaxially symmetric distributions of orientation
  - This is *not* apparent from 2-D patterns collected in a single 'projection' of shear flow.
  - Studying multiple projections (e.g. 1-2 + 1-3 planes) helps, but most of reciprocal space is still left unexplored: no guarantee that you won't miss something.
- What to do?
  - Exhaustive mapping of reciprocal space to construct full $\psi(\mathbf{u})$ ('pole figures')
    - Impractical for *in situ* studies
  - Keep limitations in mind; multiple projections where possible

'Real world' approaches to x-ray anisotropy analyses in shear

- Can simply analyze azimuthal scans using conventional order parameter analysis
  - Quantitative measure of orientation, ranges from 0 to 1
  - But, S loses its rigorous significance in relation to underlying orientation distribution function
  - Implicit assumption of uniaxial symmetry will generally be false
- Alternative metrics of orientation
  - FWHM of peaks in azimuthal scan
    - Sharper peaks: higher orientation

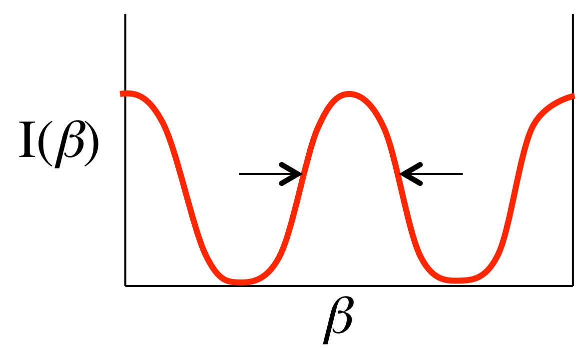

  - 2nd moment tensor analyses…

2nd moment tensor analyses of shear-induced anisotropy

Clay dispersion, 1-2 plane

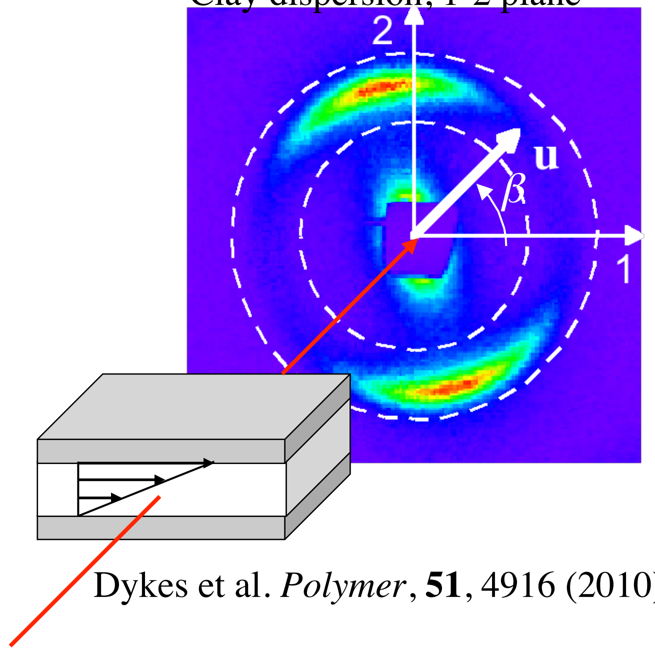

Dykes et al. *Polymer*, **51**, 4916 (2010)

Azimuthal scan, $I(\beta)$

$$u_1 = \cos\beta;\ u_2 = \sin\beta$$

$$\langle \mathbf{uu} \rangle = \begin{bmatrix} \langle u_1 u_1 \rangle & \langle u_1 u_2 \rangle \\ \langle u_1 u_2 \rangle & \langle u_2 u_2 \rangle \end{bmatrix}$$

$$\langle u_1 u_2 \rangle = \langle \cos\beta \sin\beta \rangle = \frac{\int_0^{2\pi} \cos\beta \sin\beta I(\beta)\, d\beta}{\int_0^{2\pi} I(\beta)\, d\beta}$$

<u>Anisotropy Factor</u>

$$AF = \sqrt{\left(\langle u_1 u_1 \rangle - \langle u_2 u_2 \rangle\right)^2 + 4\langle u_1 u_2 \rangle^2}$$

<u>Orientation Angle</u>

$$\chi = \frac{1}{2}\tan^{-1}\left(\frac{2\langle u_1 u_2 \rangle}{\langle u_1 u_1 \rangle - \langle u_2 u_2 \rangle}\right)$$

Cinader & Burghardt *J Polym Sci Part B Polym Phys*, **37**, 3411 (1999)

Practical considerations: Everything is easier at a synchrotron

- High flux
  - Facilitates rapid data acquisition; real-time studies
  - Detectors important, too
- Intrinsic collimation
  - High quality SAXS
- Tunable energy/ wavelength
  - Can facilitate shear cell construction

Advanced Photon Source, ANL

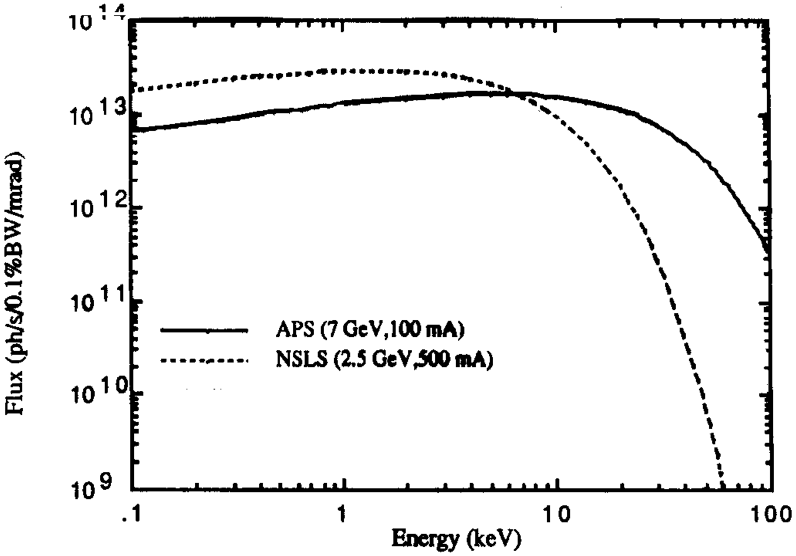

X-ray absorption and energy

- 'Lab' x-ray sources operate at ~ 8 keV (1.54 Å)
- APS specializes in 'hard' x-rays (higher energy)
- Consider change in absorption between 8 and 25 keV:

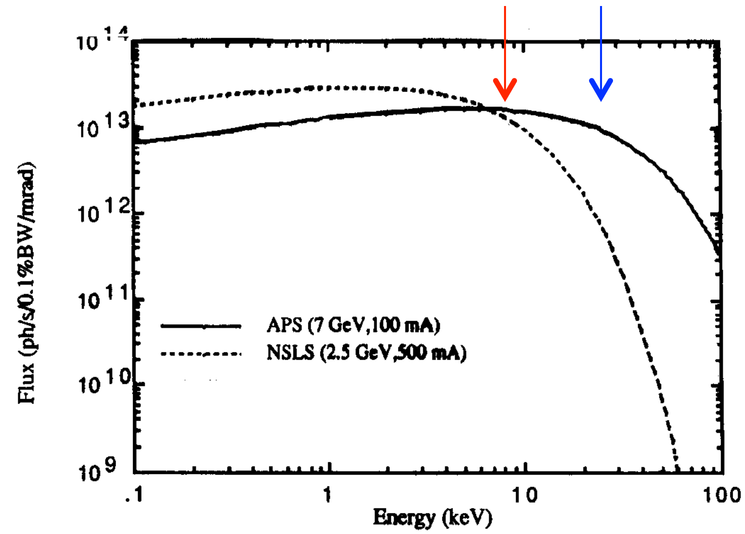

Material	Transmission, 8 keV	Transmission, 25 keV
1 mm polycarbonate	51.8 %	96.5 %
50 µm mica	54.4 %	97.8 %
1 mm silicon	6×10^{-5} %	60.5 %
1 mm aluminum	2×10^{-4} %	63.9 %

http://henke.lbl.gov/optical_constants/filter2.html

X-ray shear cell 'window' materials

Material	X-ray Absorption	Background scattering	Mechanical strength
Kapton® (polyimide film)	Low	Faint diffraction at q = 0.5 Å^{-1}; SAXS background	Flexible; use as supported thin film
Mica	Manageable for thin sheets	Good for both SAXS & WAXS (avoid Bragg condition)	Stiffer, but fragile; use as supported thin film
Polycarbonate	Manageable	Good for SAXS; broad amorphous scattering a problem in WAXS	Good; ease of fabrication for complex shapes (solvent?)
Silicon	Requires high energy	Negligible in WAXS (avoid Bragg condition)	Good
Aluminum	Requires high energy	Need to mask WAXD at q ≥ 2.7 Å^{-1}; grain structure gives SAXS at low q.	Good; ease of fabrication for complex shapes

X-ray shear cell construction: Couette (1-3 & 2-3 planes)

- Pople *et al*., *Rev. Sci. Inst.* 69, 3015 (1998)
  - Thin polycarbonate
  - 1-3 plane (radial) only
- Panine *et al*., *Rev. Sci. Inst.* 74, 2451 (2003)
  - Thin polycarbonate or aluminum (high energy only)
  - 1-3 or 2-3 planes
  - Integrated with rheometer
  - 10 – 170˚C

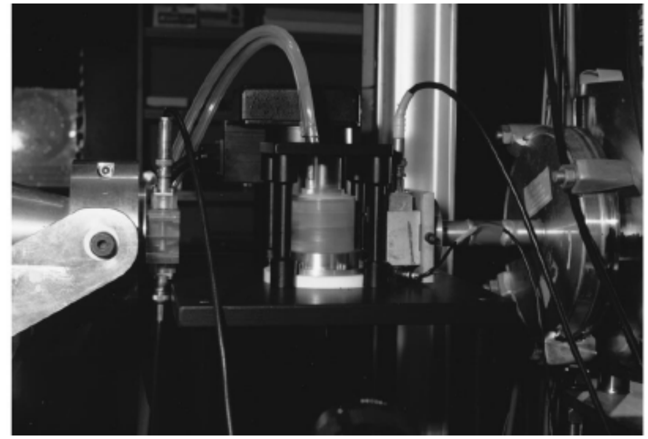

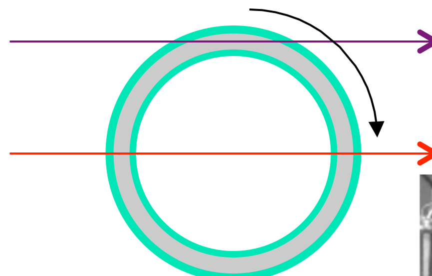

X-ray shear cell construction: Rotating disk (1-3 plane)

- Frequent use of supported mica or Kapton windows
  - Solutions
    - Keates *et al*. *Polymer,* **34**, 1316 (1993)
    - Hongladarom *et al*. *Macromolecules*, **29**, 5346 (1996)
    - Münch and Kalus, *Rev. Sci. Inst.*, **70**, 187 (1999)
  - Melts
    - Gervat *et al*. *Phil. Trans. Roy. Soc. Lon*. A, **350**, 1 (1995)
    - Ugaz and Burghardt, *Macromolecules*, **31**, 8474 (1998)

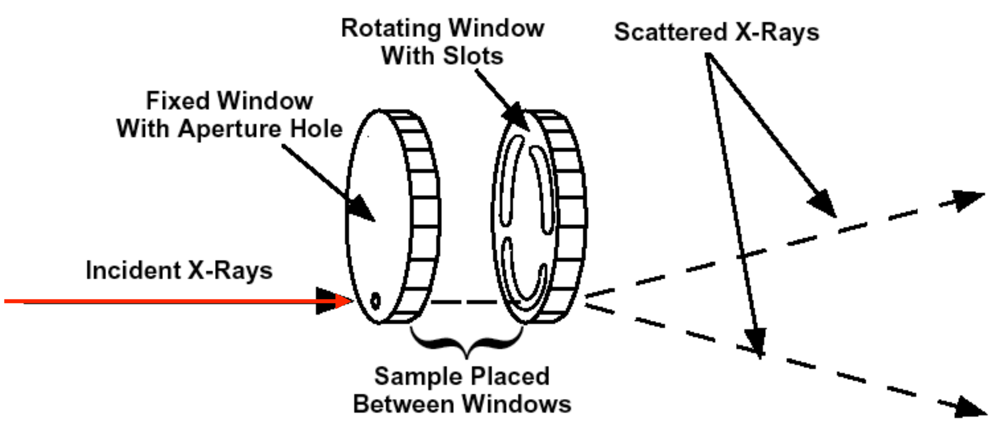

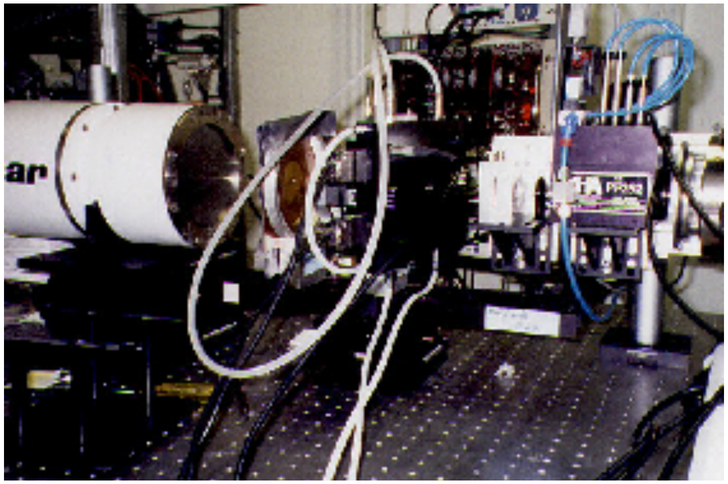

X-ray shear cell construction: Annular cone & plate (1-2 plane)

- Caputo & Burghardt, *Macromolecules*, **34**, 6684 (2001)
- Solutions or melts
- Steady or oscillatory

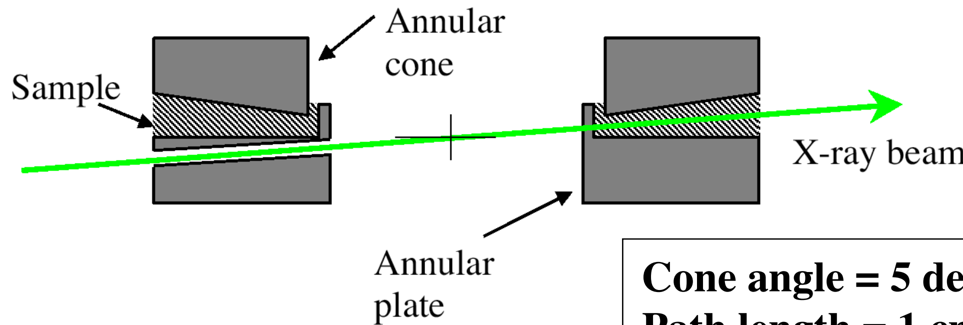

Cone angle = 5 deg
Path length = 1 cm

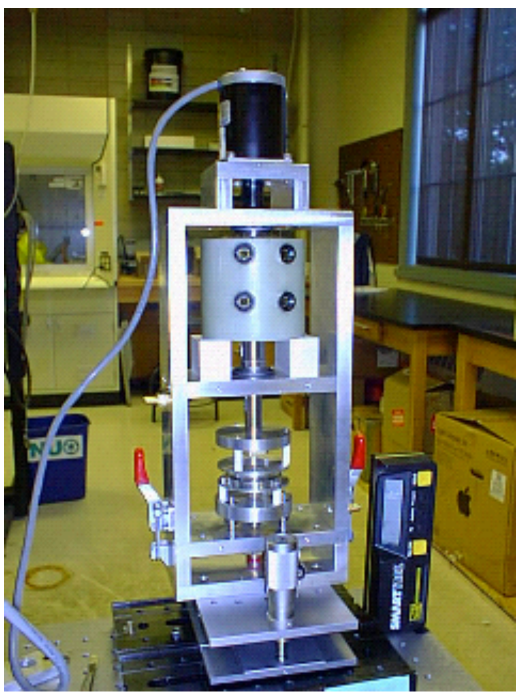

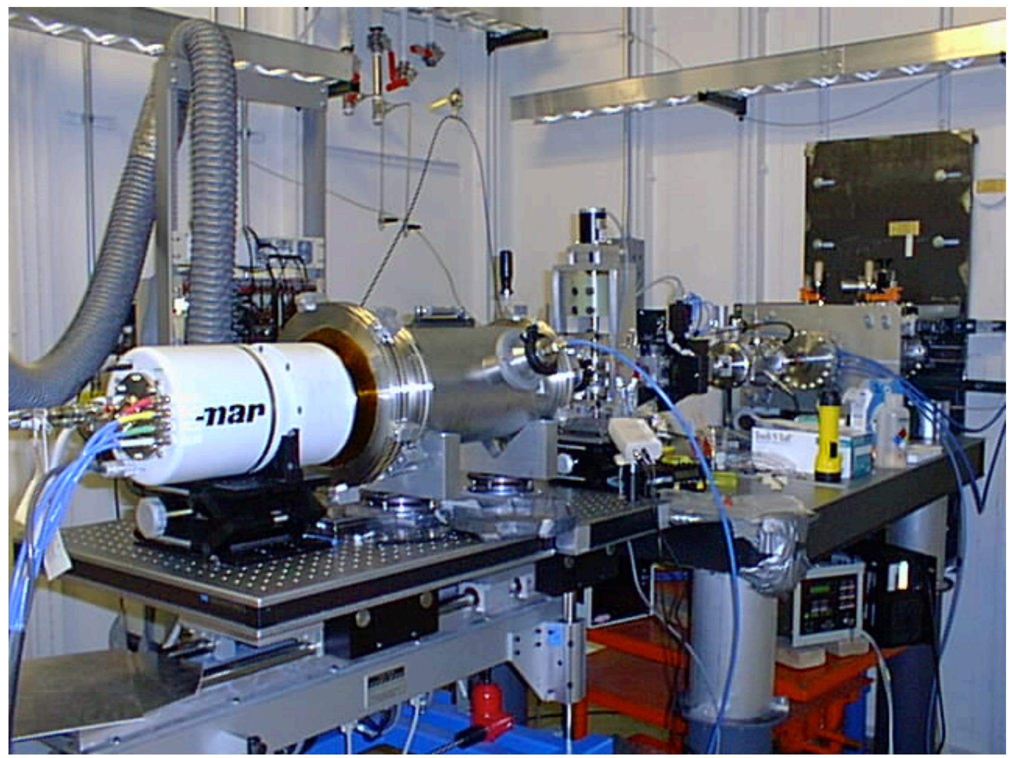

Case study 1: Liquid crystalline polymers

Rigid rod LCP sol'n; 1-3 plane:

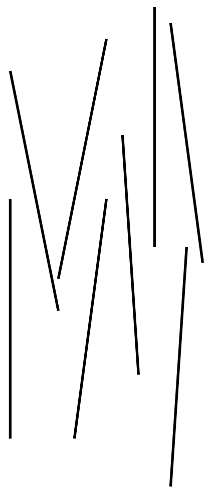

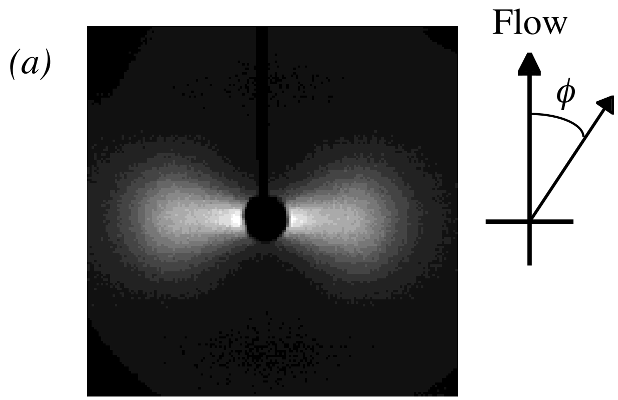

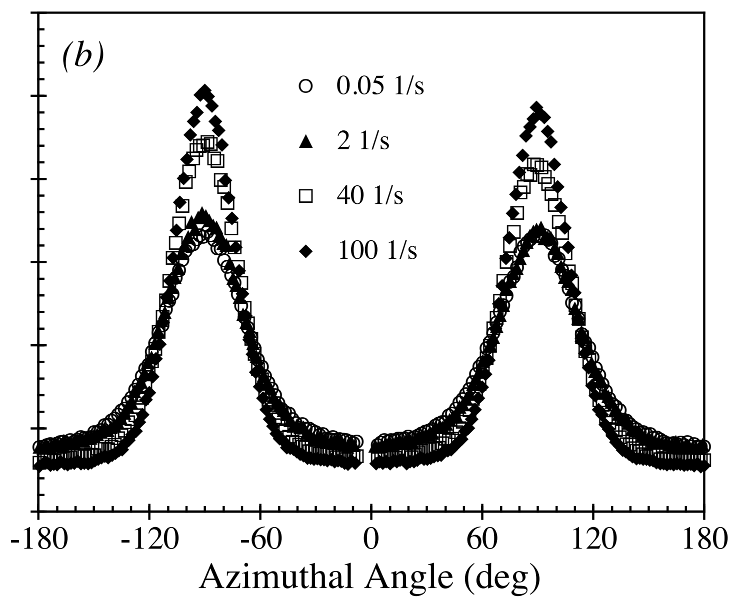

Burghardt, *Macromol. Chem. Phys.* 199, 471 (1998)

Semiflexible LCP melt; 1-3 plane:

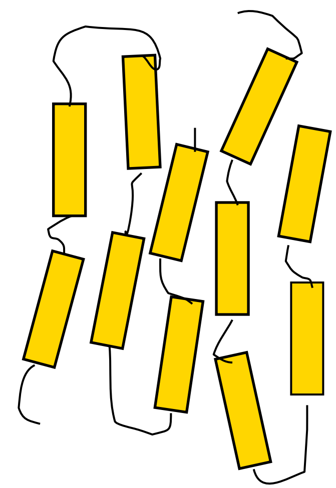

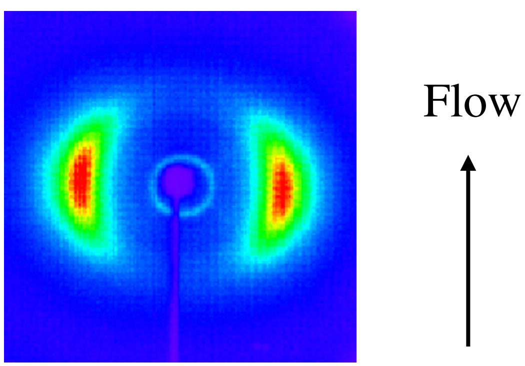

Ugaz et al., *JOR*, **45**, 1029 (2001)

Lyotropic poly(benzyl glutamate) solution, 1-2 plane

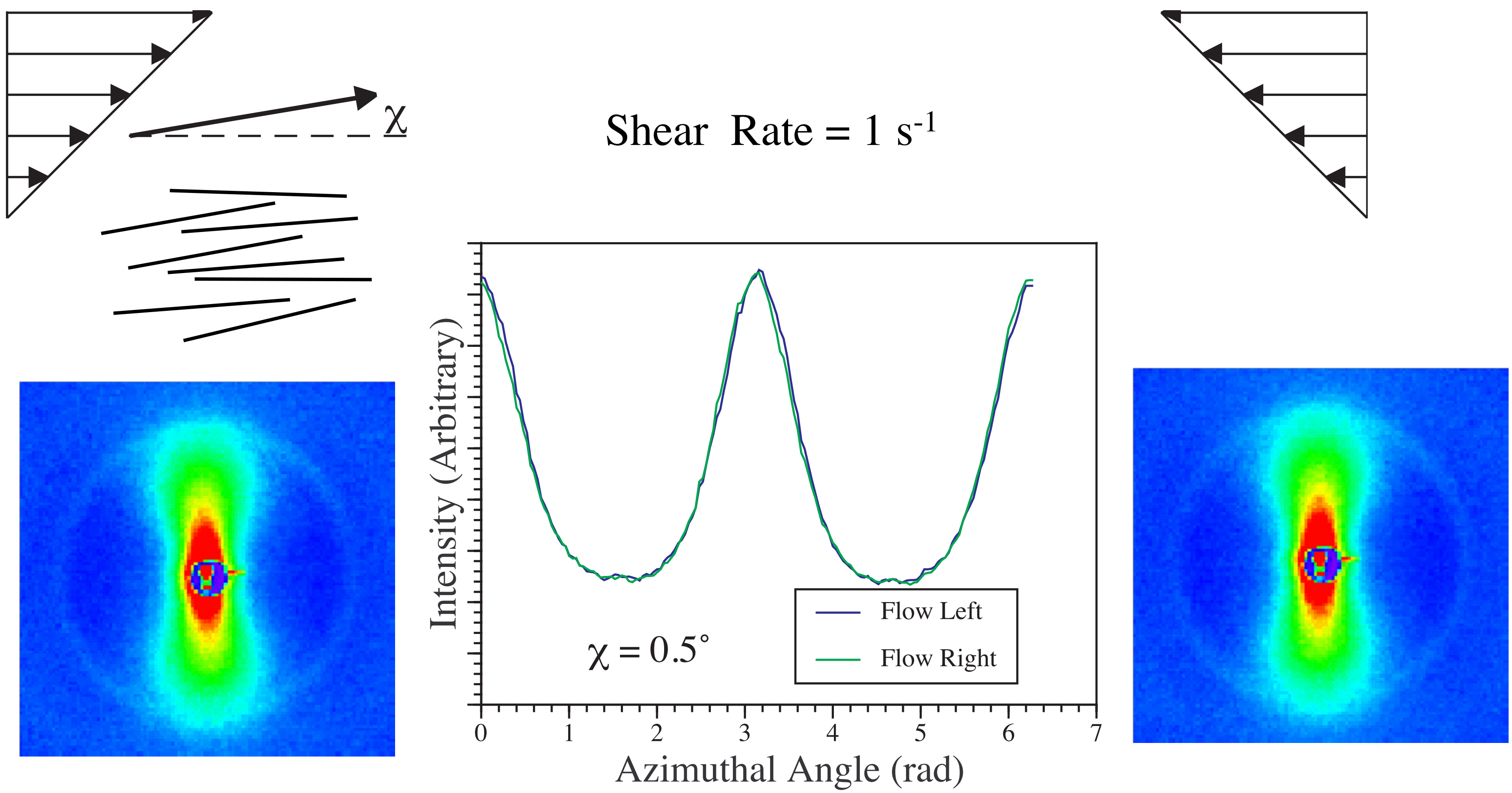

Caputo & Burghardt, *Macromolecules*, 34, 6684 (2001).

Lyotropic poly(benzyl glutamate) solution, steady state orientation

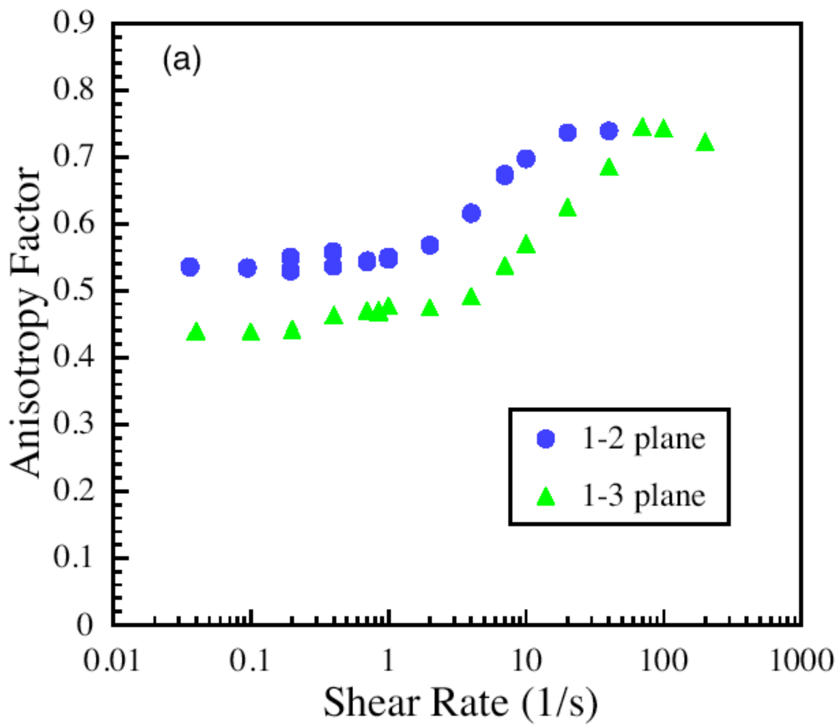

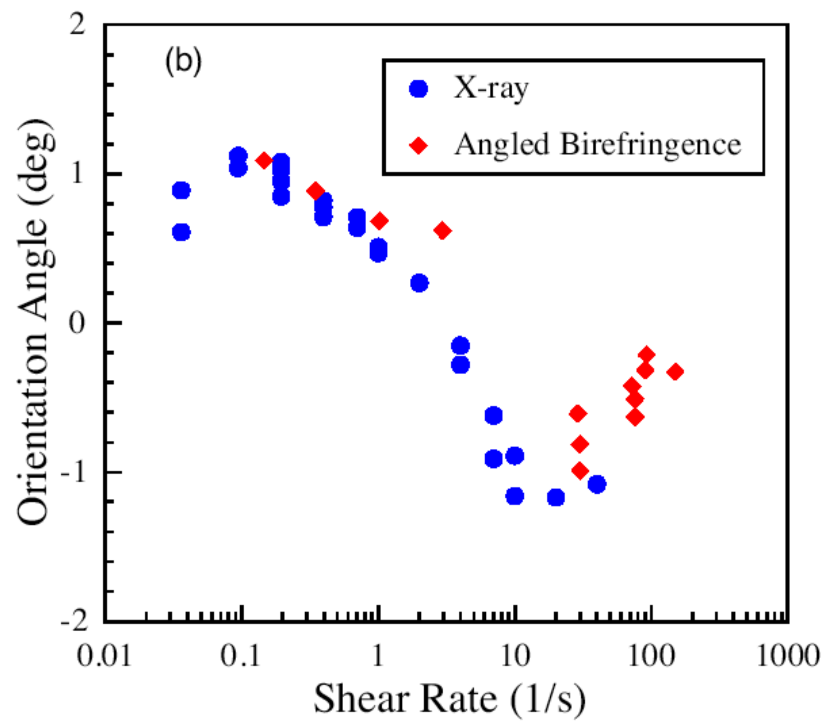

- ‘Tumbling’ to ‘shear-aligning’ transition
- Macroscopically biaxial orientation state at low rates
- Sign change in angle predicted by molecular theories

Caputo & Burghardt, *Macromolecules*, 34, 6684 (2001).

Lyotropic poly(benzyl glutamate) solution, transient orientation dynamics

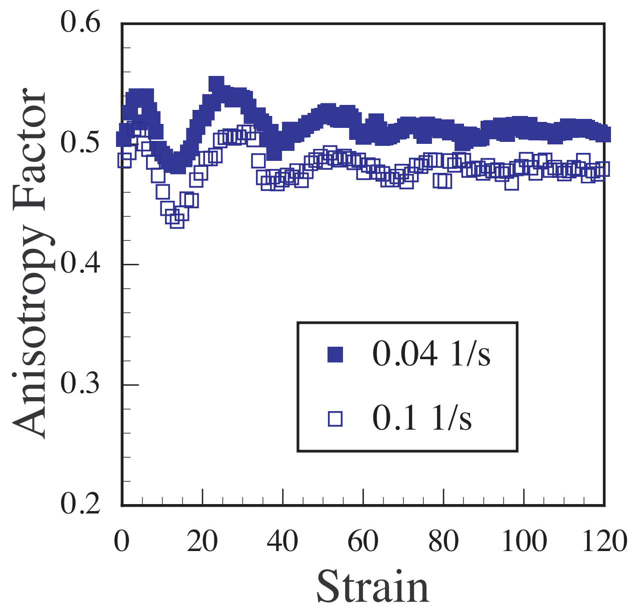

Shear flow reversal

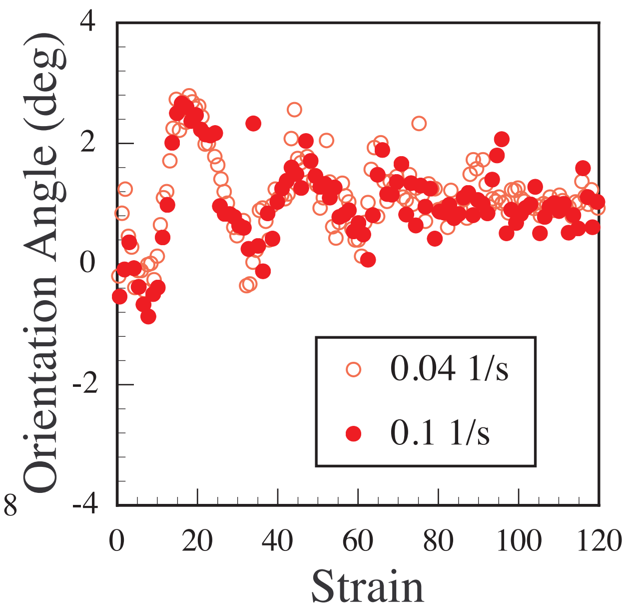

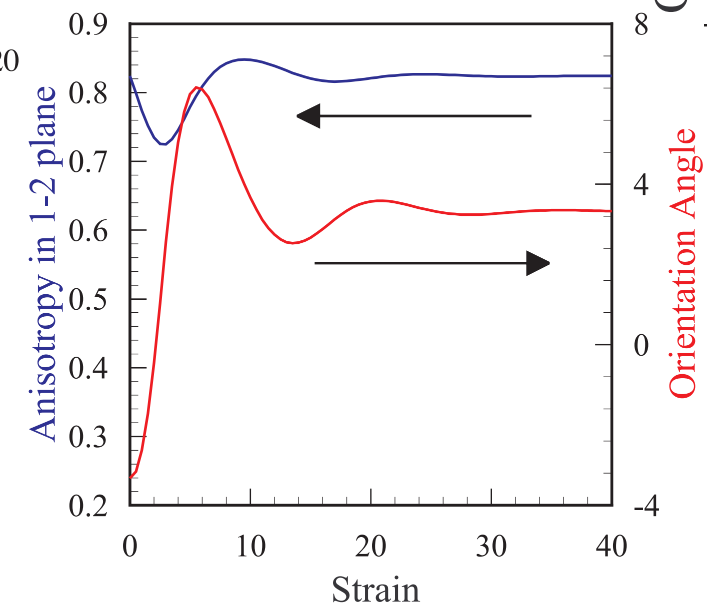

(Larson-Doi 'tumbling polydomain' model)

Caputo & Burghardt, *Macromolecules*, 34, 6684 (2001).

Thermotropic DHMS-7,9 melt Orientation development in start-up

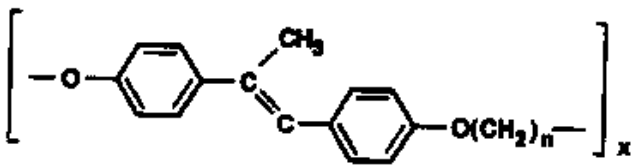

DHMS-7,9:
Known to be ‘shear aligning’ (Kornfield)

Clear into isotropic phase → cool into nematic phase → random ‘polydomain’ IC

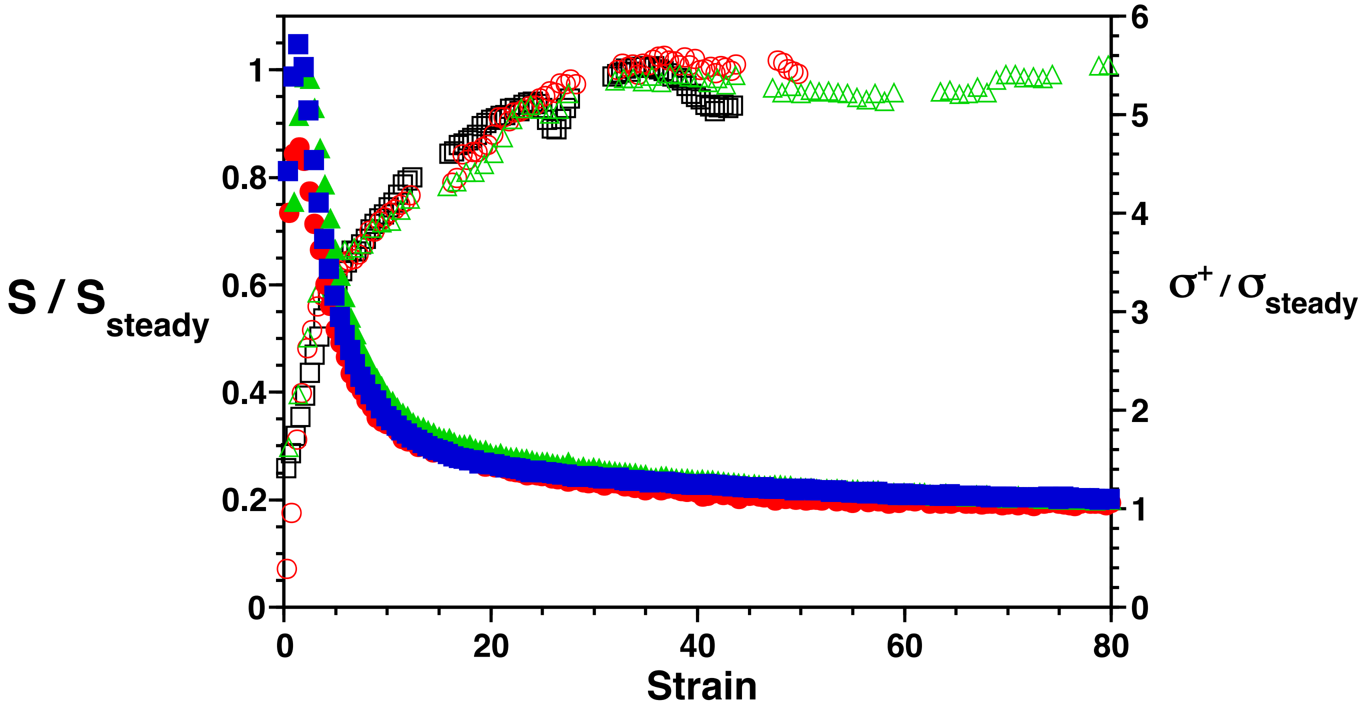

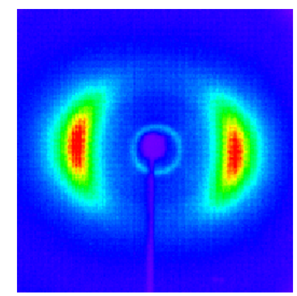

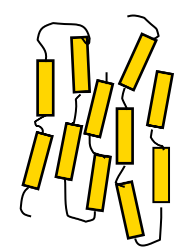

Ugaz *et al*., *J. Rheol*. **45**, 1029 (2001)

Thermotropic DHMS-7,9 melt
'Polydomain' modeling

$$\frac{\partial \mathbf{n}}{\partial t} = \mathbf{n}\cdot\boldsymbol{\omega} - \lambda(\mathbf{n}\cdot\mathbf{D} - \mathbf{nnn}\cdot\mathbf{D})$$

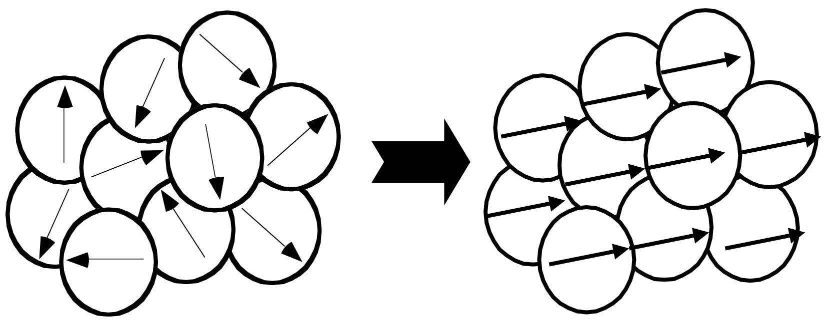

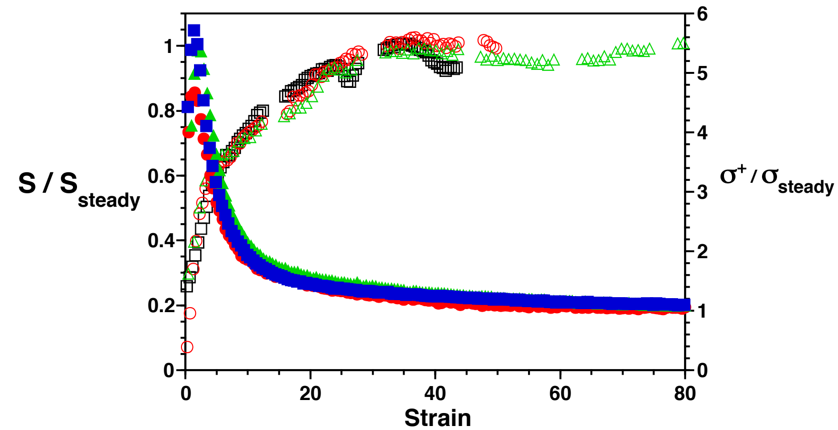

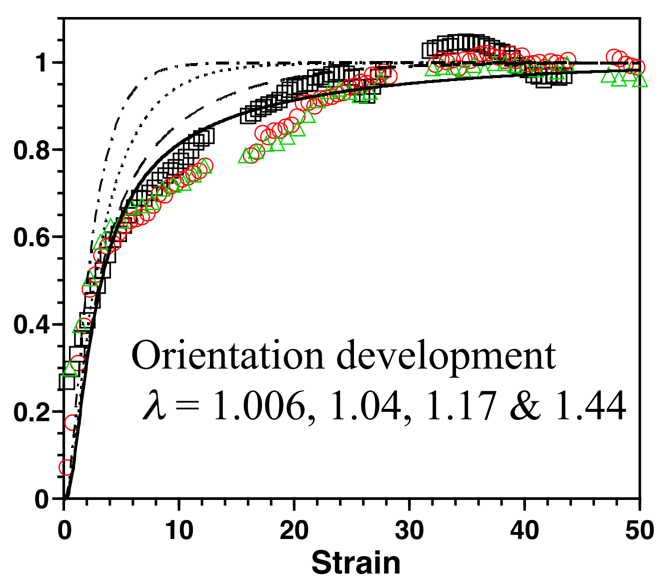

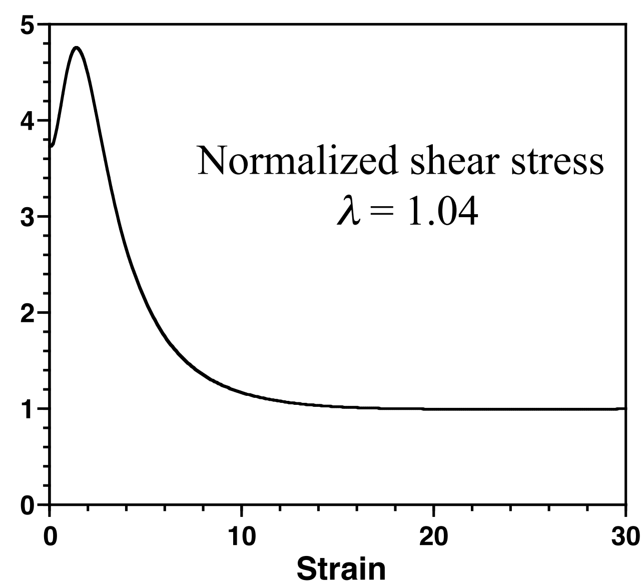

Ugaz *et al*., *J. Rheol*. **45**, 1029 (2001)

Smectic side-chain LCP: Large-amplitude oscillatory shear

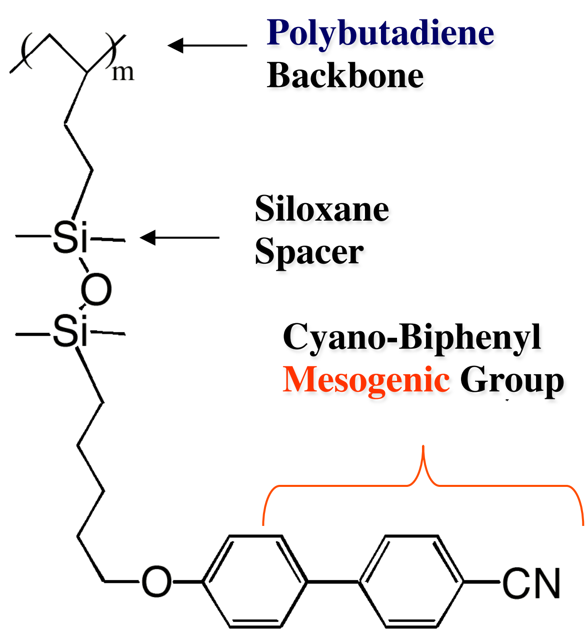

SCLCP Nomenclature:

PBSiCB5

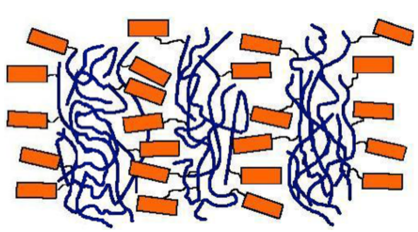

1-3 plane SAXS

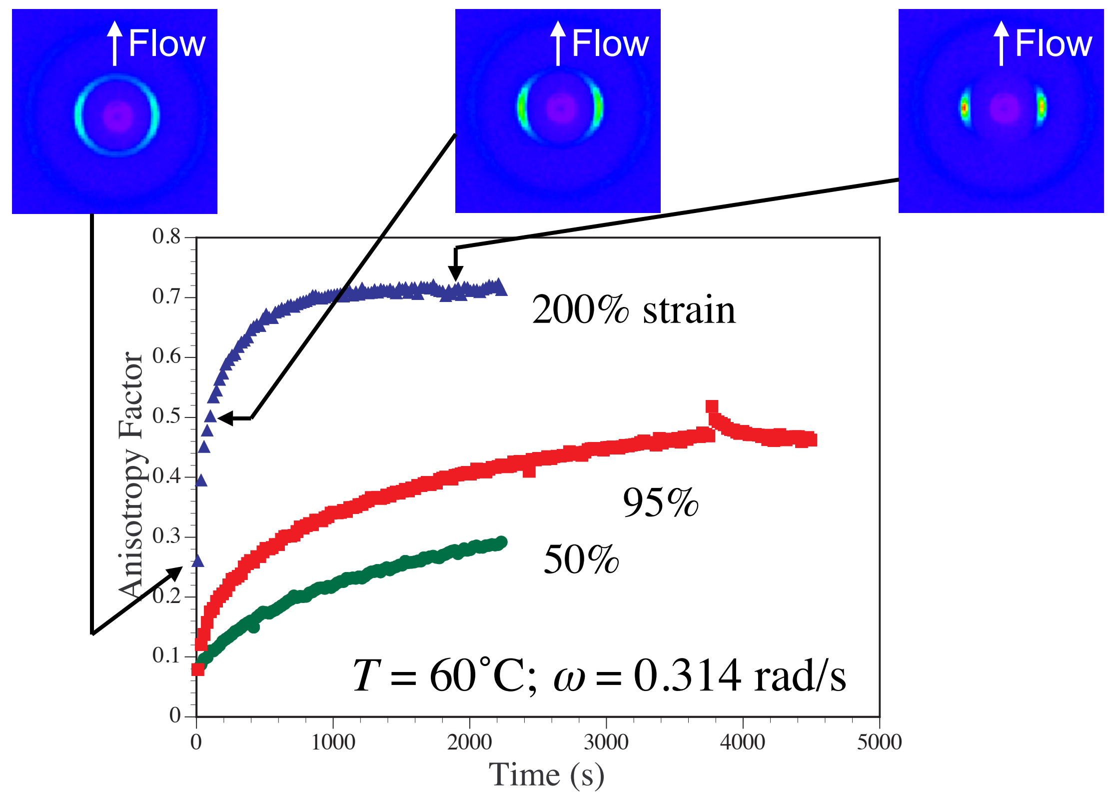

Auad *et al*., Macromolecules, 38, 6946 (2005)
Rendon *et al*., *Macromolecules*. **40**, 6624 (2007)

Case study 2: Block copolymers

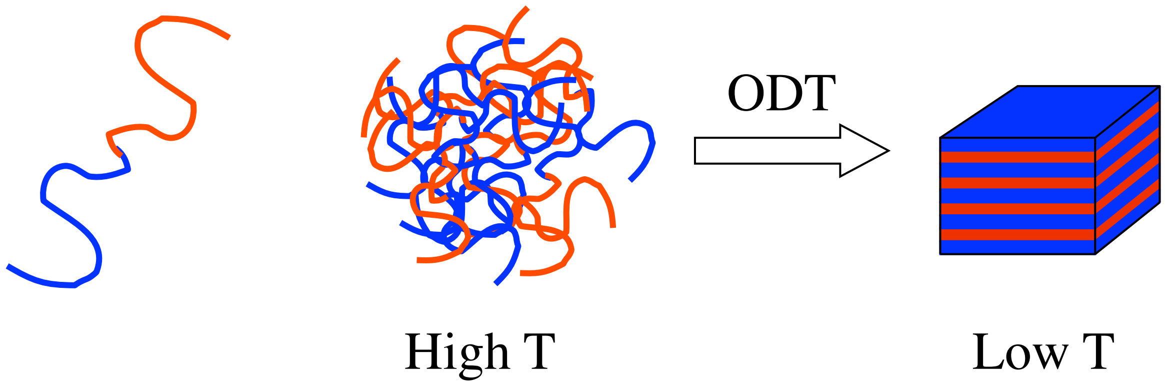

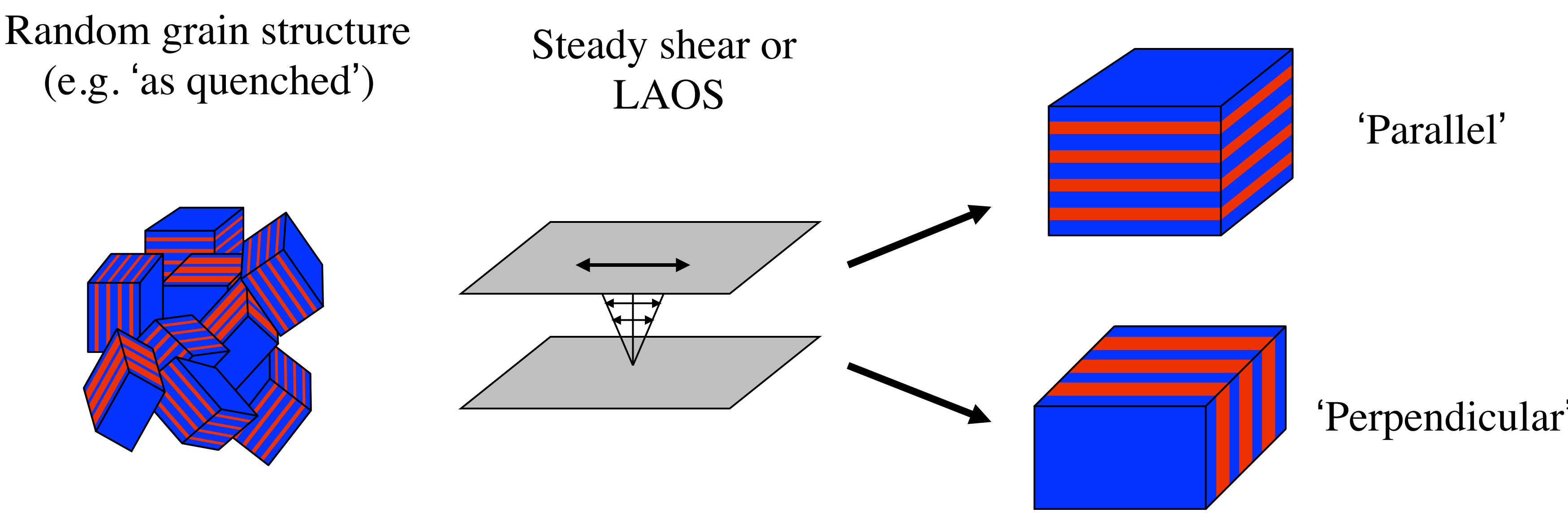

PS-PI lamellar diblock: Inception of shear flow

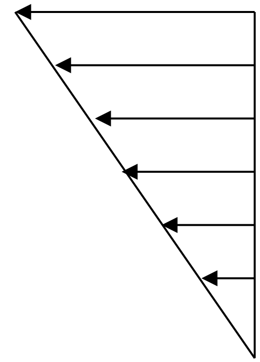

- M = 20,850
- f_{PS} = 0.49
- ODT = 170˚C
- Studied at 115˚C; 1-2 plane

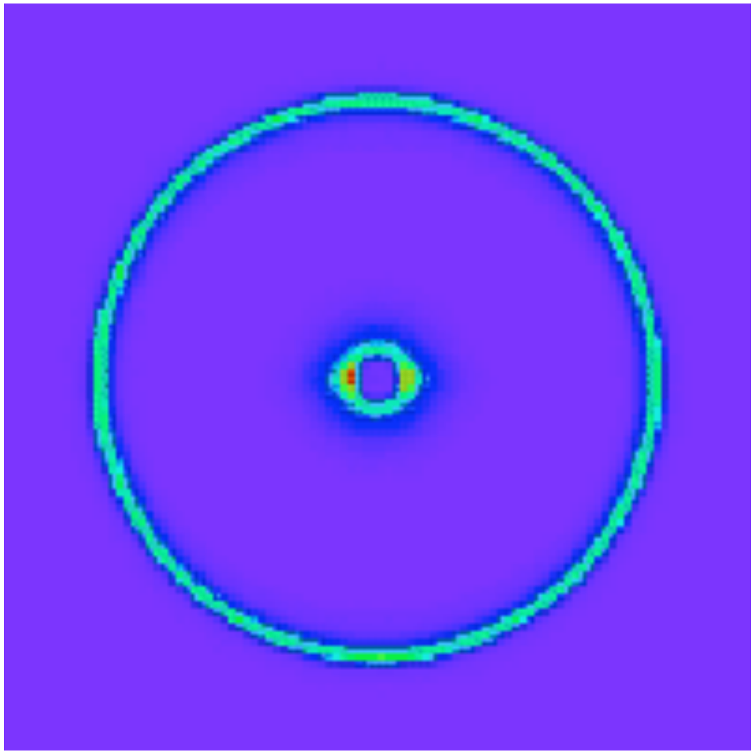

- Shear Rate: 0.03 s^{-1}
- Video sequence sped up by factor of 35. (~1 sec/strain unit)
- Flow from *right* to *left*.

F. E. Caputo, PhD thesis

PS-PI lamellar diblock: Test of 'grain rotation' model

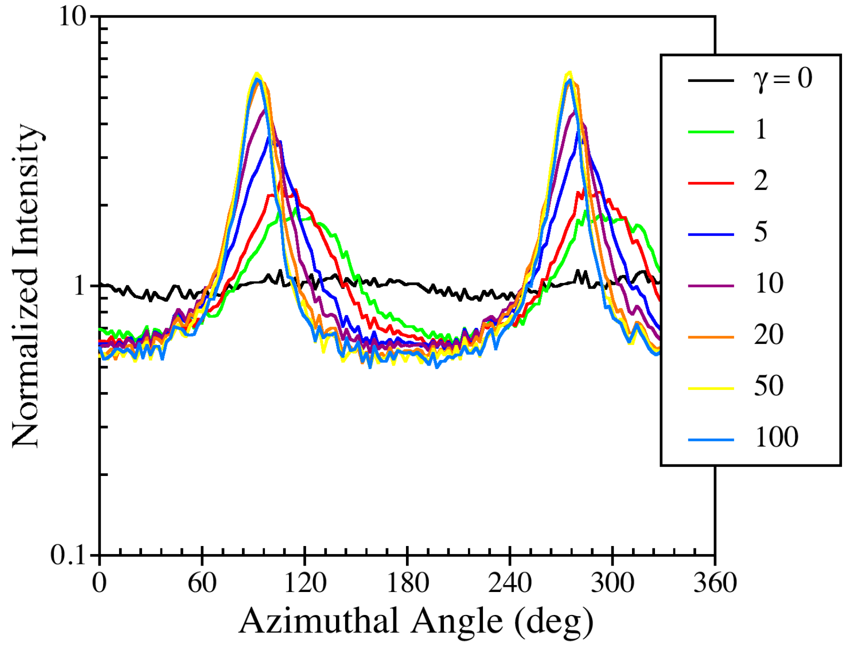

Grain rotation predictions:

D. Polis *et al.*, *Macromolecules*, **32**, 4668 (1999)

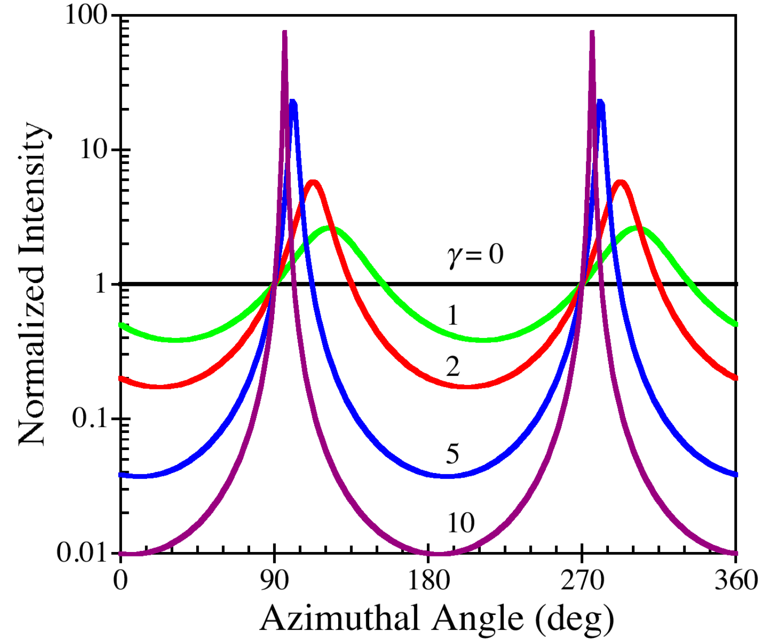

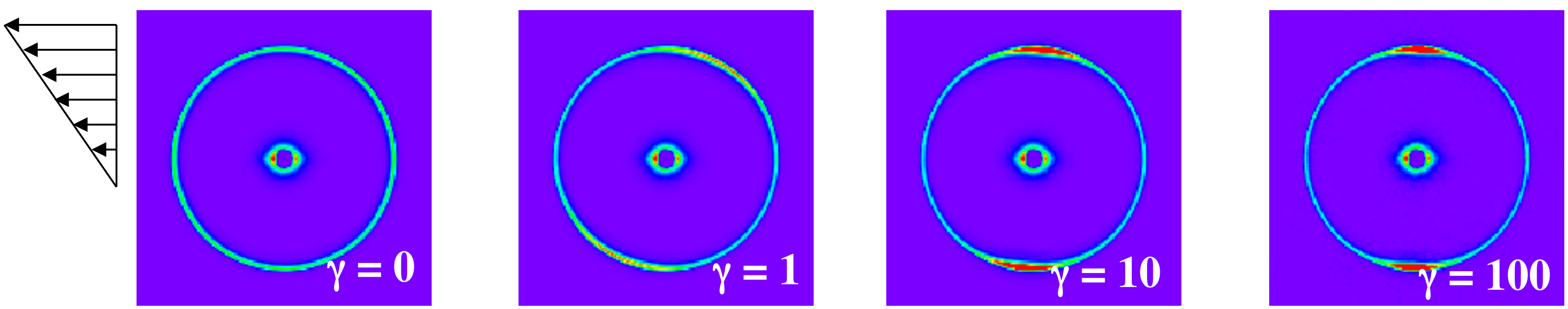

F. E. Caputo, PhD thesis

PS-PI lamellar diblock: Multiple projections of shear

‘1-2’ plane

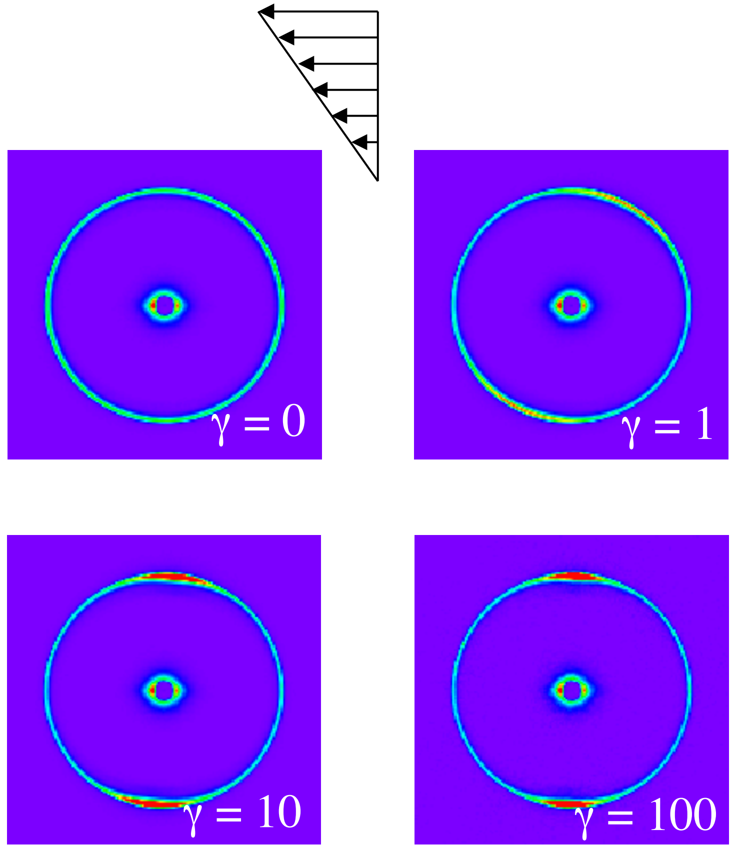

Looks ‘parallel’

‘1-3’ plane

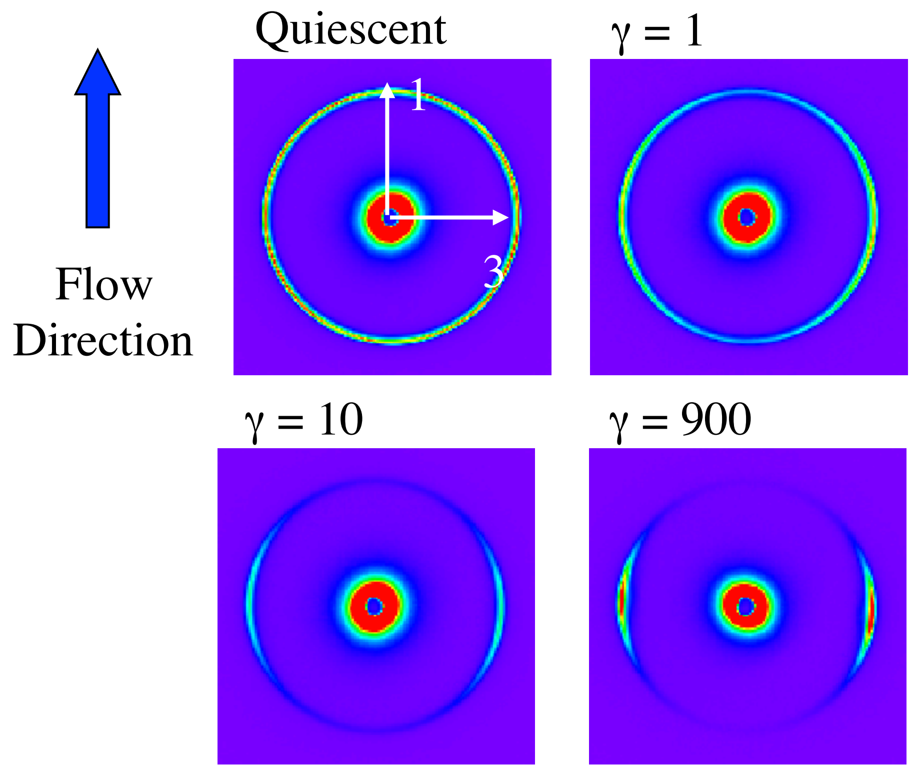

Looks ‘perpendicular’

F. E. Caputo, PhD thesis

Case study 3: Polymer nanocomposites

- Organoclay in polybutene (intercalated)
- Measurements in 1-2 plane

Shear flow at 1 s^{-1}

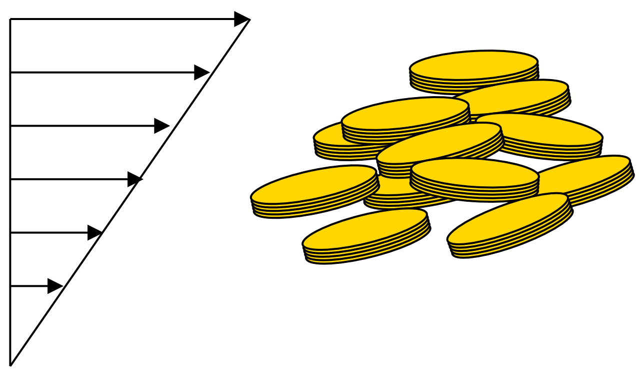

WAXS:

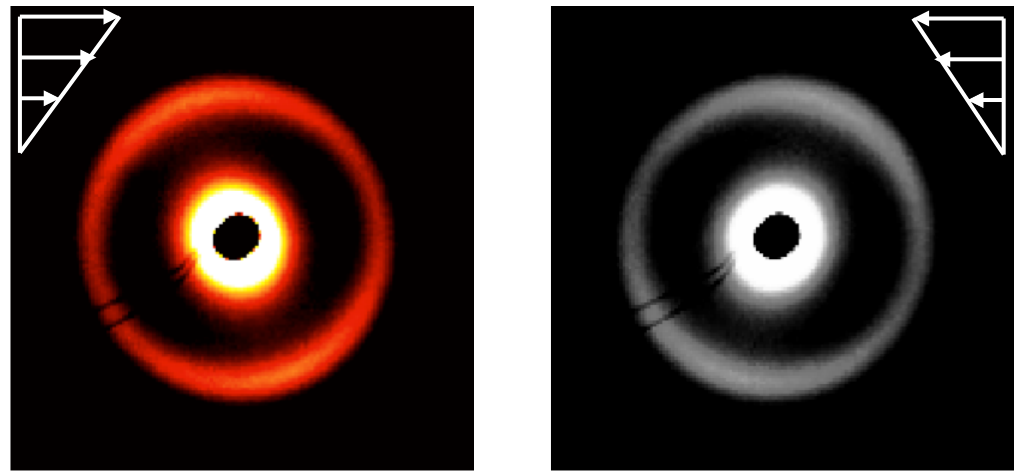

SAXS:

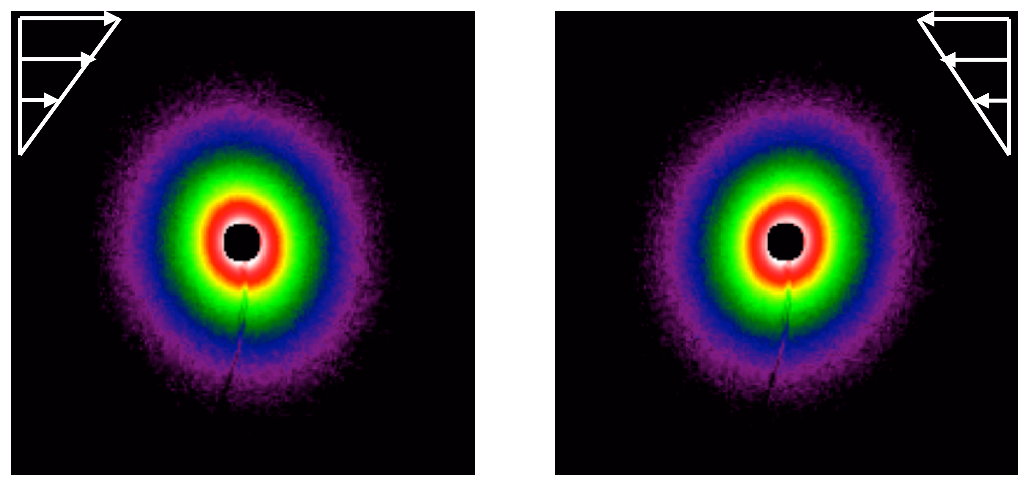

S. Pujari *et al.*, *Rheol. Acta*, **50**, 3 (2011)

Clay/polybutene dispersion: Steady state orientation & rheology

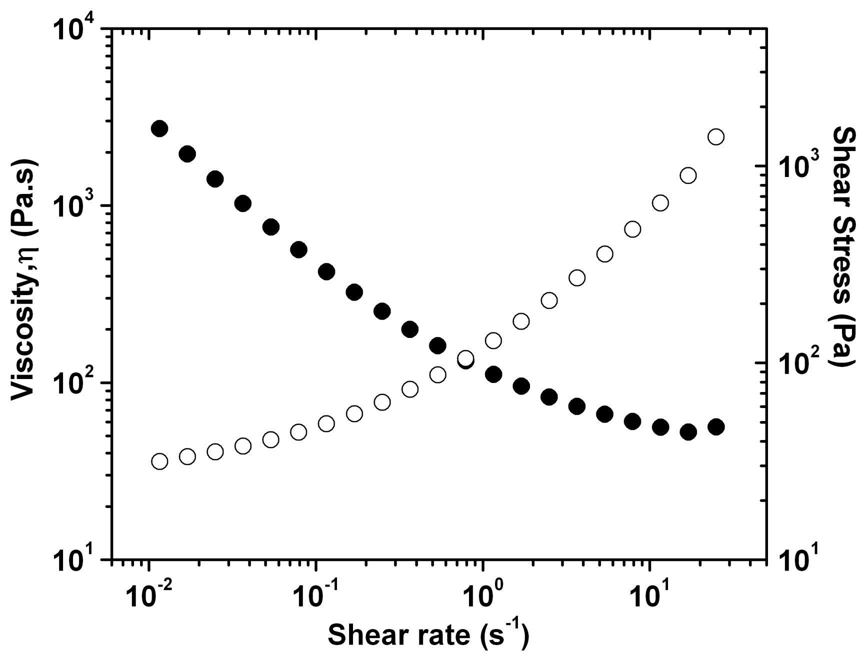

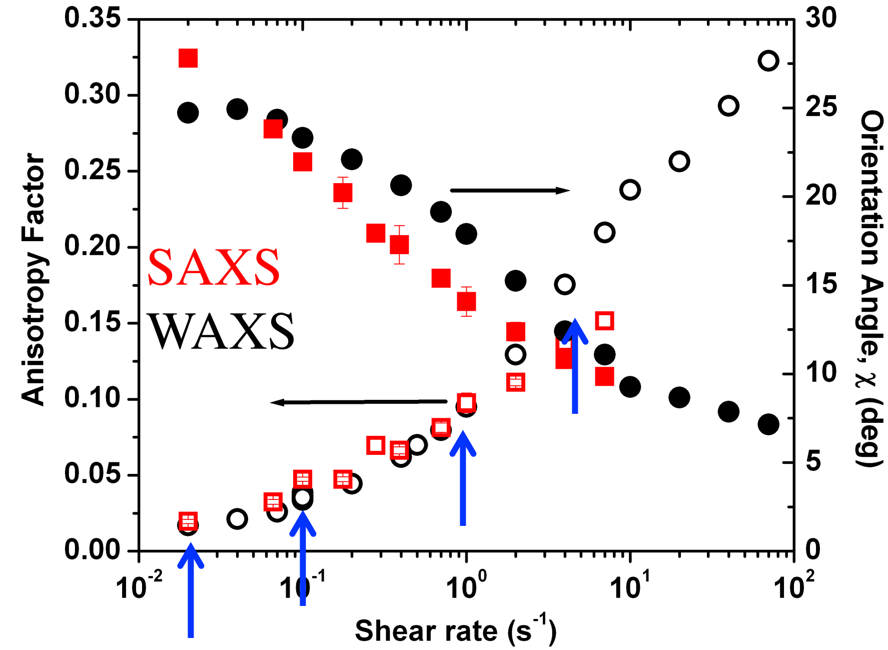

- Low rates (~ 0.01 s^{-1}): negligible orientation & yielding
- Orientation development with increasing shear rate
- Consistent with estimated $D_r \sim 0.003\ s^{-1}$

S. Pujari *et al.*, *Rheol. Acta*, **50**, 3 (2011)

Clay/polybutene dispersion: Relaxation phenomena

Mechanical:

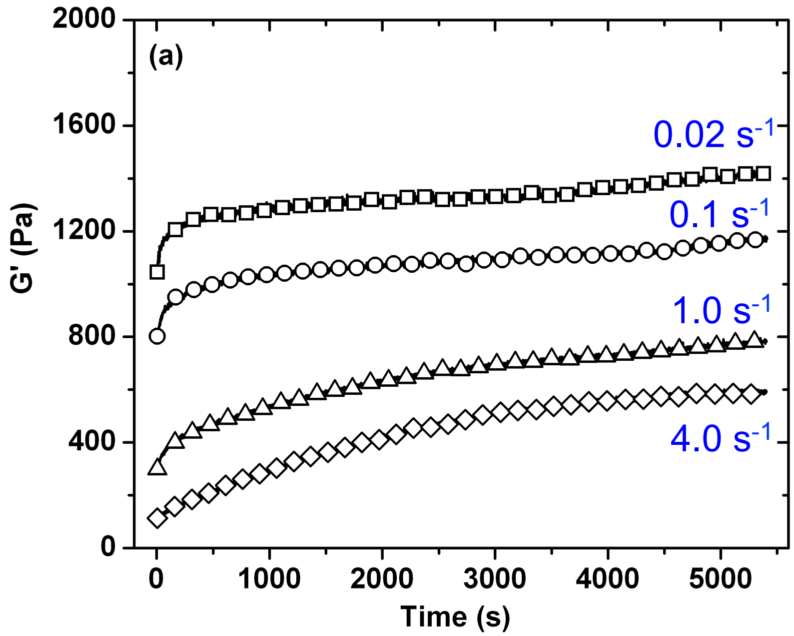

Structural:

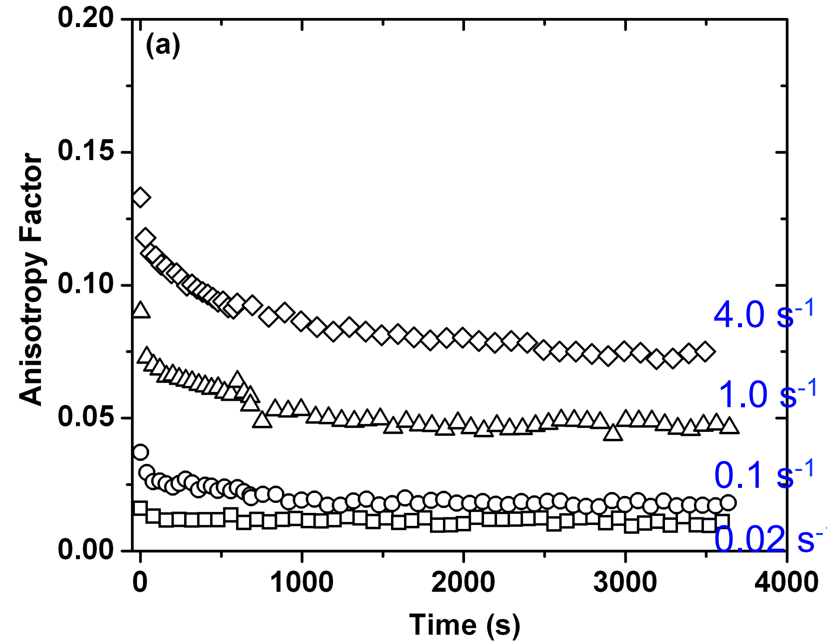

- Low rates: not much change in either alignment or *G'*
- Higher rates: partial relaxation of orientation; greater changes in *G'*
- Similar time scales for particle relaxation & *G'* recovery

S. Pujari *et al.*, *Rheol. Acta*, **50**, 3 (2011)

Multi-walled carbon nanotube dispersions

Optical microscopy & SAXS in 1-3 plane

- $L = 40\ \mu\mathrm{m}$, $d = 50$ nm
- Dispersed in uncured epoxy
- 0.05 wt%

- Mixture of single tubes and aggregates
- Higher shear rates– aggregate break-up
- Associated development of SAXS anisotropy in 1-3 plane

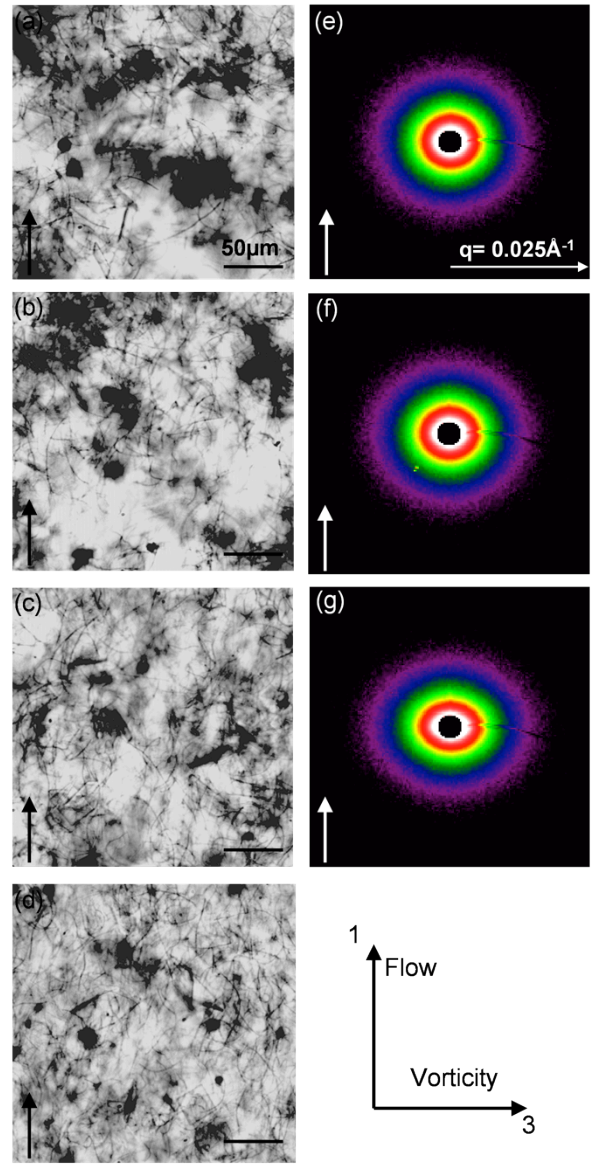

0.02 s^{-1}

0.2 s^{-1}

2.0 s^{-1}

20 s^{-1}

S. Pujari *et al*., *J. Chem. Phys*, **130**, 214903 (2009)

0.05 wt% MWCNT dispersion: 1-2 plane

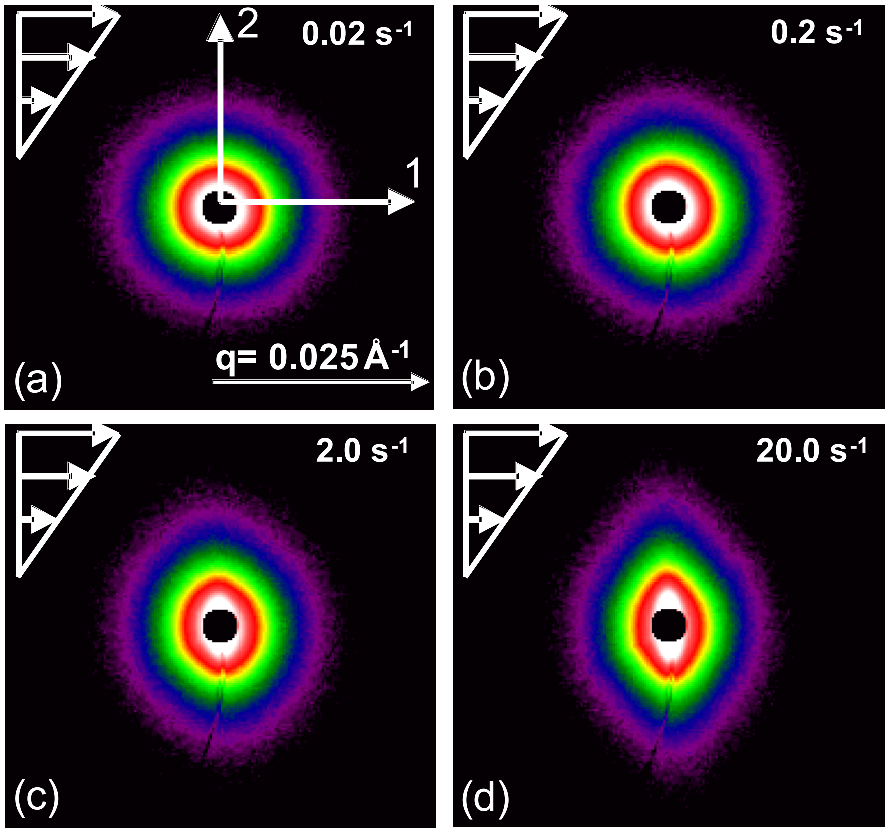

- Negligible anisotropy at low rates
- Increasing anisotropy with increased shear rate
- Orientation direction tends towards, but doesn't reach, flow direction at higher rates.

S. Pujari *et al*., *J. Chem. Phys*, **130**, 214903 (2009)

0.05 wt% MWCNT dispersion: Steady state orientation

[Open: 0.05 wt% Filled: 0.1 wt%]

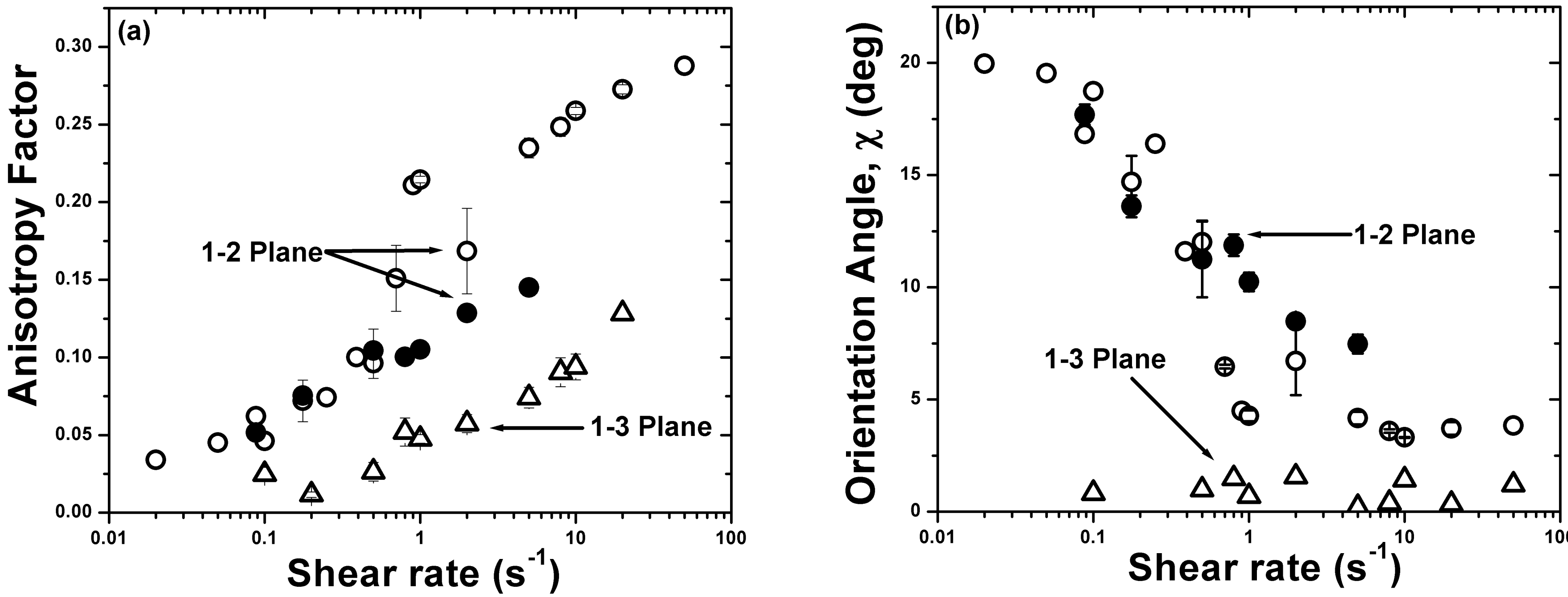

- Higher anisotropy in 1-2 than in 1-3 plane; *not* uniaxially symmetric
- Slightly lower anisotropy, similar orientation angle for 0.1 wt% sample as compared to 0.05 wt% sample

S. Pujari *et al*., *J. Chem. Phys*, **130**, 214903 (2009)

Processing: Fiber spinning

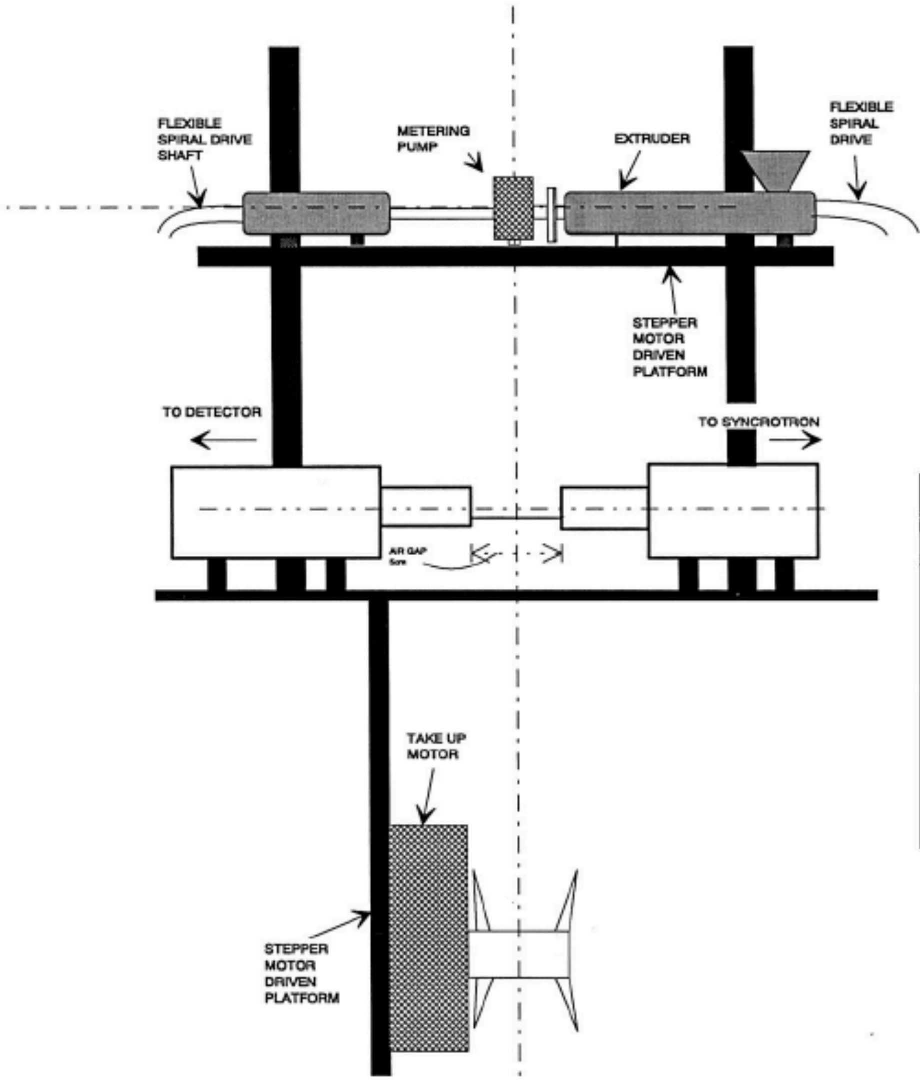

Figure 1. Melt spinning assembly.

Poly(vinylidene fluoride) fiber spinning

SAXS (top) and WAXS (bottom) patterns collected at different positions along fiber during spinning:

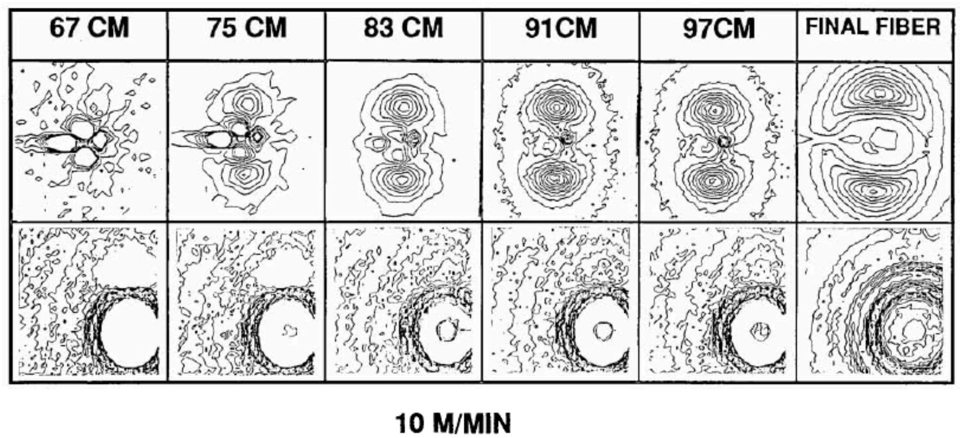

Cakmak *et al*., *J. Polym. Sci. Part B Polym. Phys.*, **31**, 371(1993)

Processing: Extrusion-fed channel flow

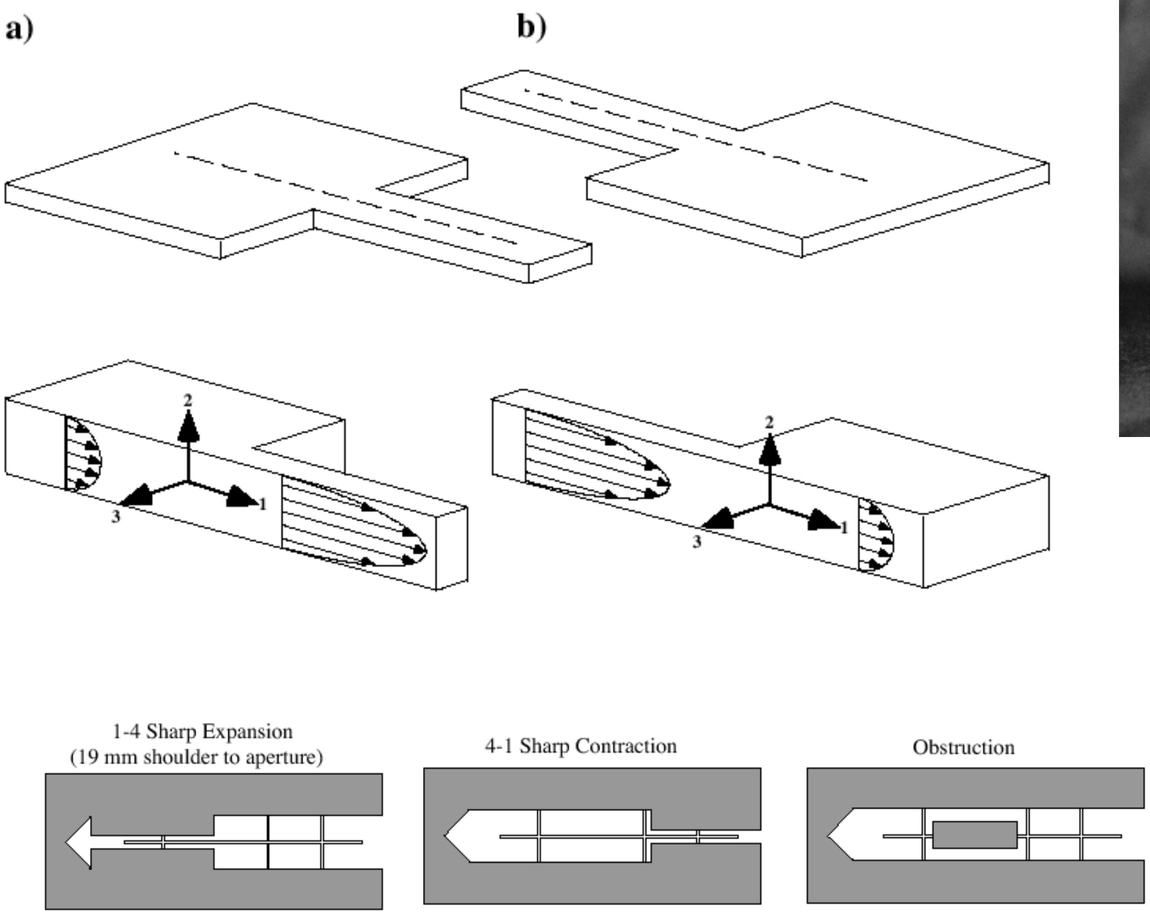

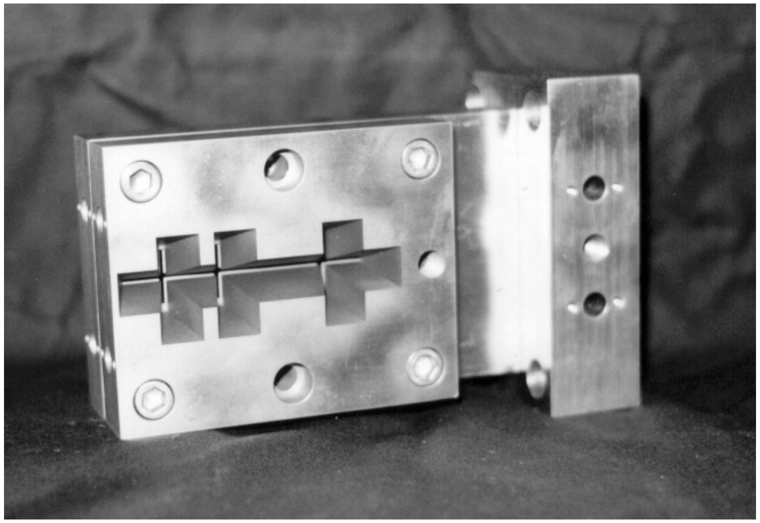

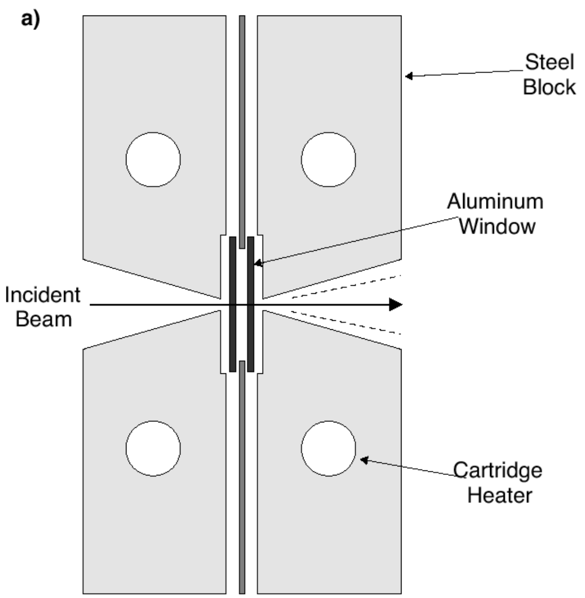

Cinader & Burghardt *Macromolecules*, **31**, 9099 (1998)

Extrusion experiment

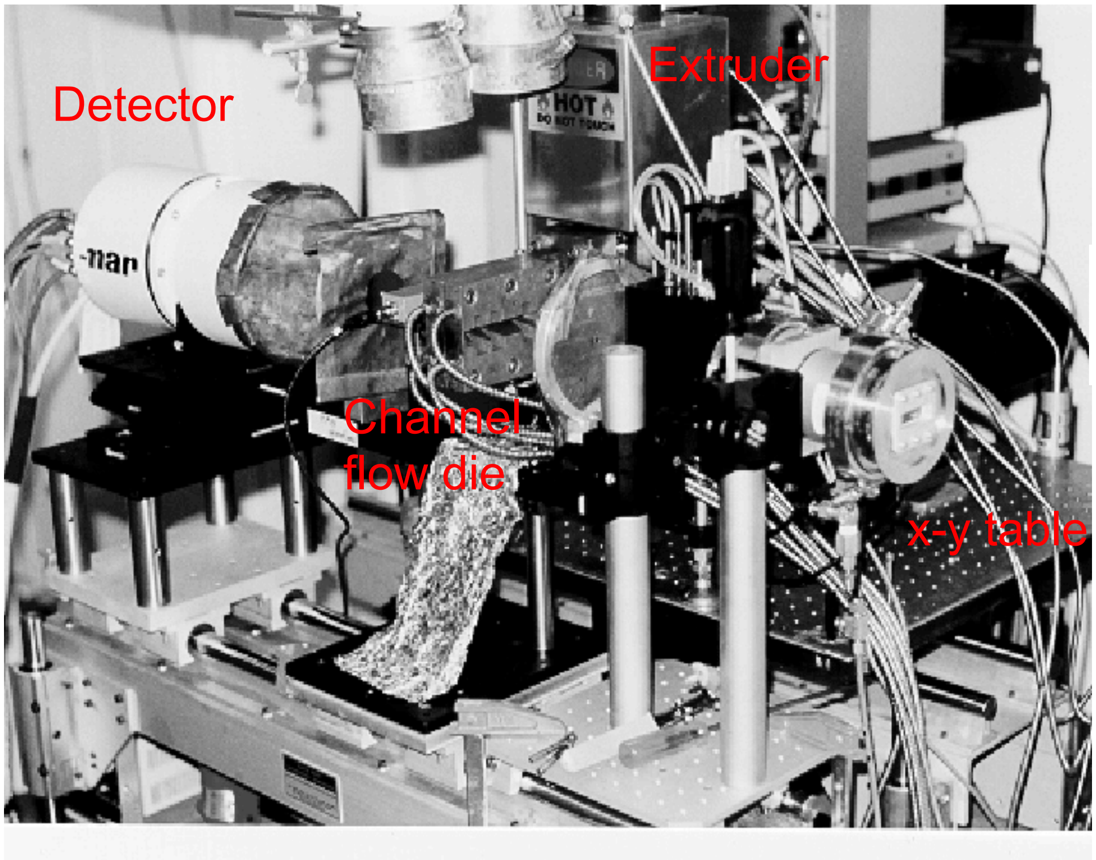

- Xydar® commercial LCP

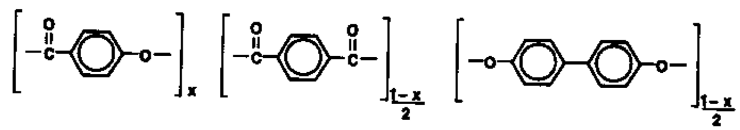

- Melt experiments at 350 C

Cinader & Burghardt *Macromolecules*, **31**, 9099 (1998)

LCP orientation in slit-contraction flow

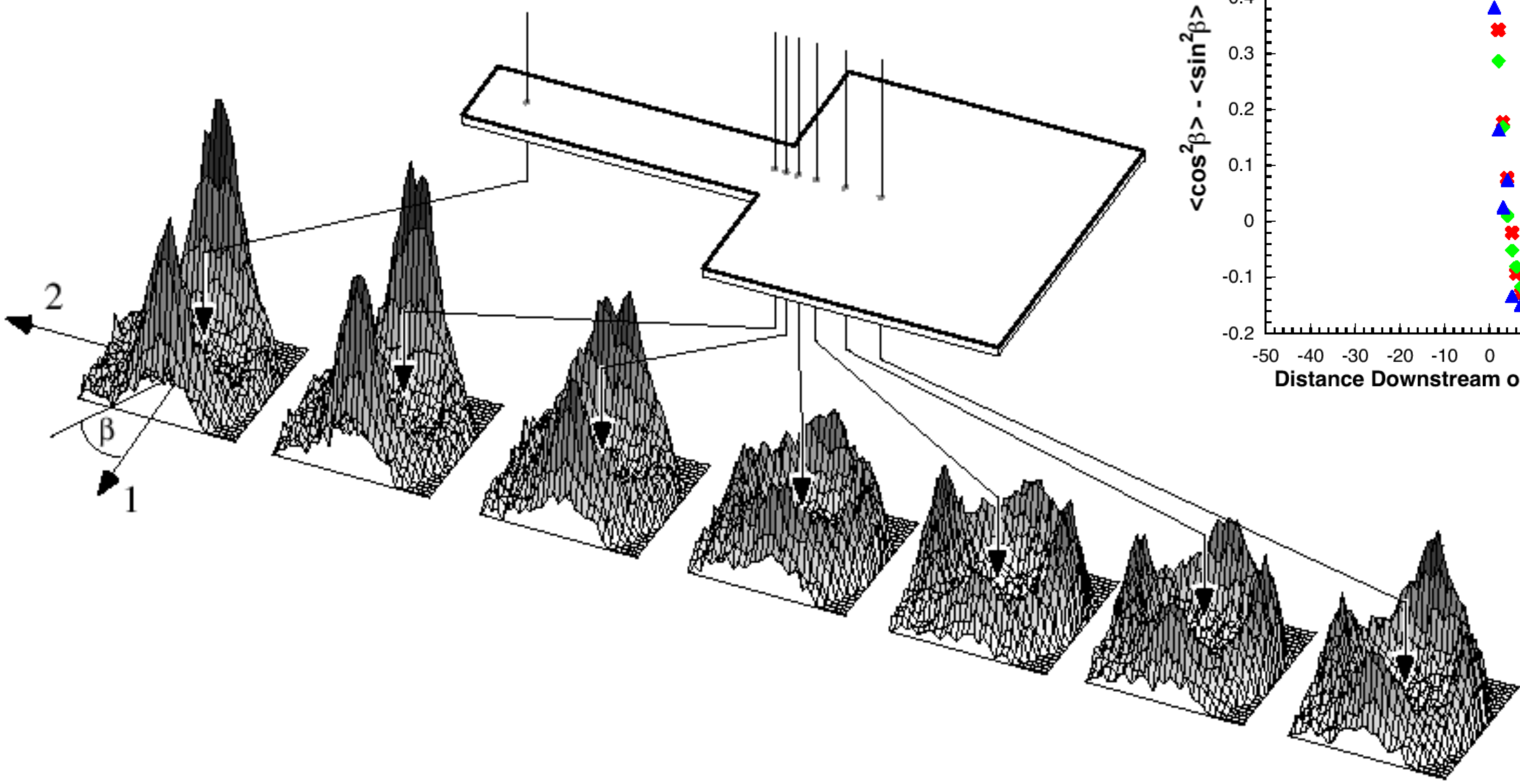

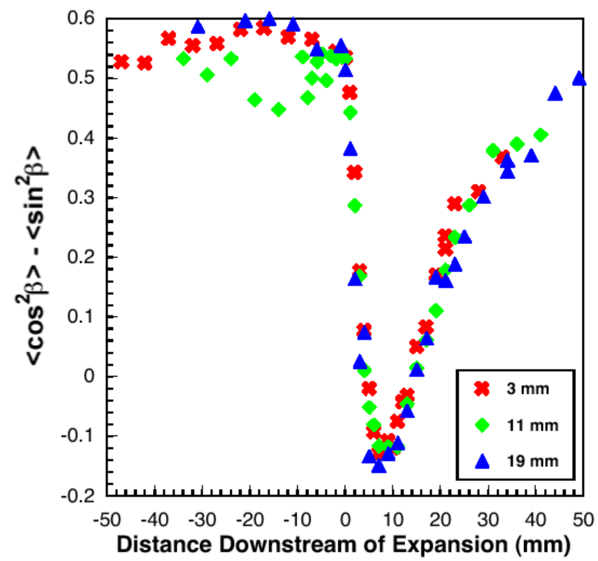

Cinader & Burghardt *Macromolecules*, **31**, 9099 (1998)

Processing: Injection molding

WAXS Mold + Detector
(*Close up*)

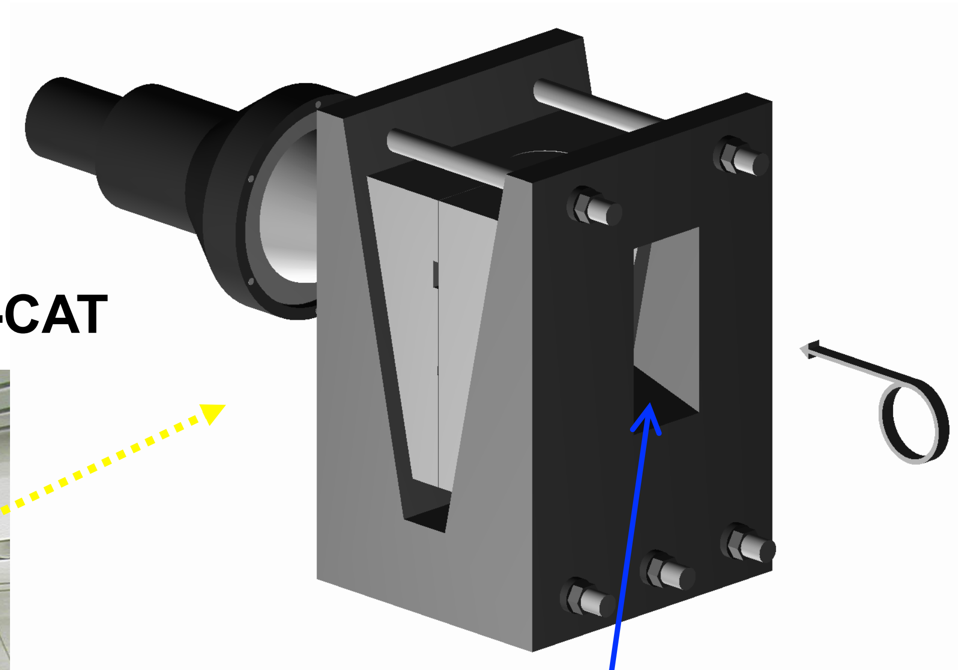

Undulator Beamline 5ID-D of DND-CAT

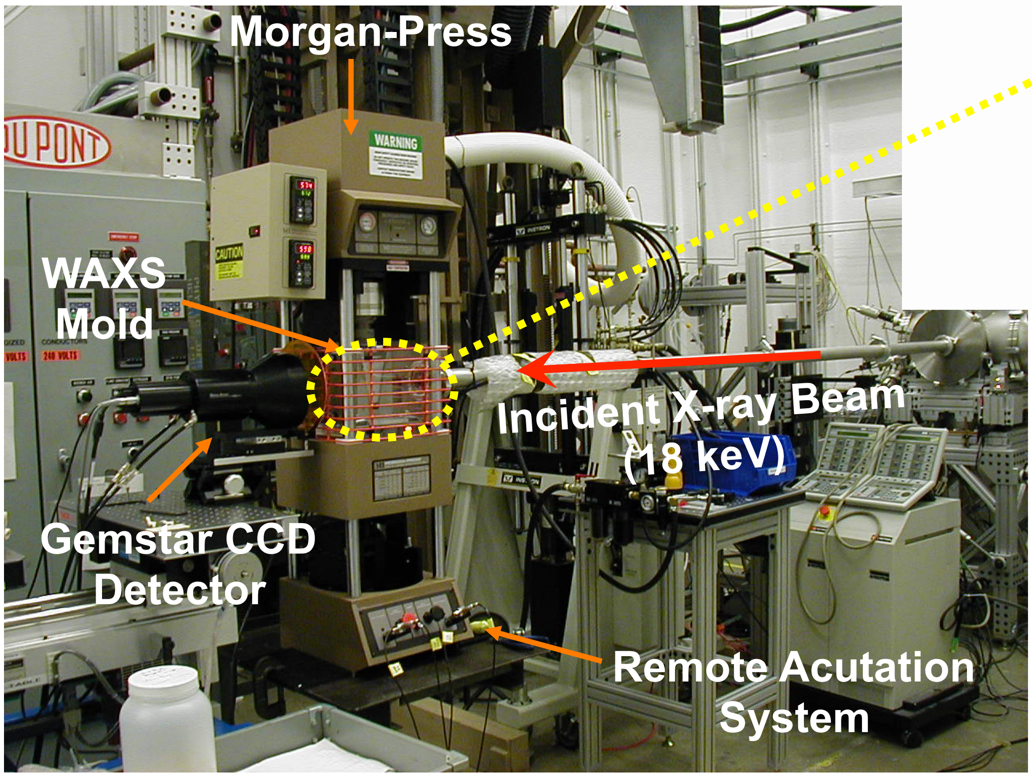

- 16° trenches (on both the mold and wedge block) allow for scattered X-rays to readily exit the mold

Rendon *et al*., *Rev. Sci. Instrum.* **80**, 043902 (2009)

X-ray injection mold tooling details

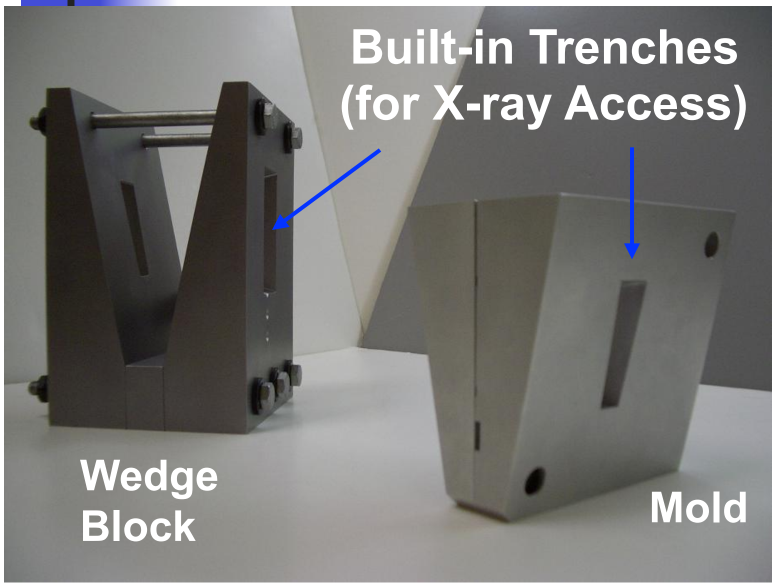

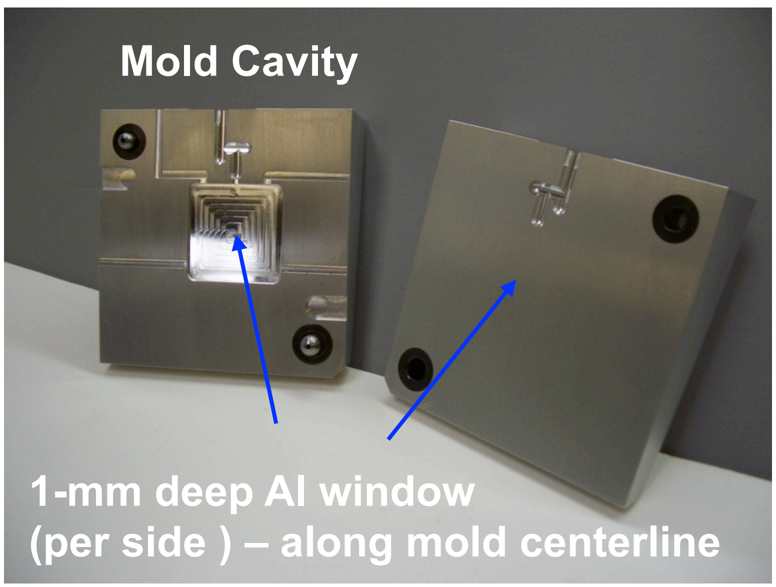

Assembled X-ray Mold
& Wedge Block
(side view)

Tie Bars

Rendon *et al*., *Rev. Sci. Instrum.* **80**, 043902 (2009)

Time-resolved measurements of orientation in TLCP molding

Vectra A® copolyester

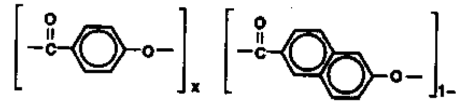

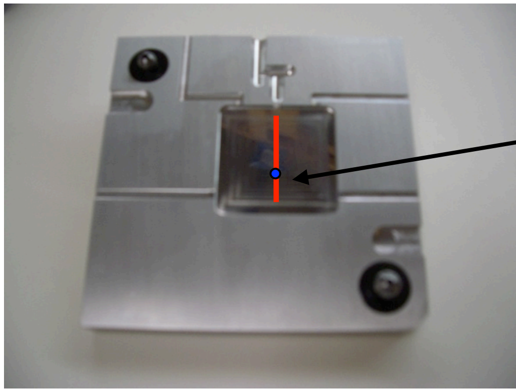

Location along mold:

23 mm away from die entrance

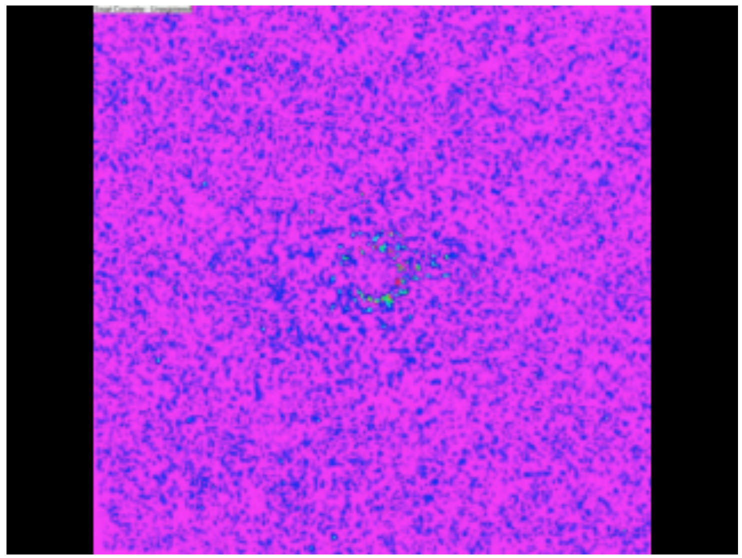

Filling Direction

Molding Parameters:

Fill time = 4 sec

T_{melt} = 285 °C

T_{nozzle} = 300 °C

T_{mold} = 90 °C

Data acquisition rate: 12 frames/sec

Video clip slowed down by factor of 2.4

Rendon *et al*., *Rev. Sci. Instrum.* **80**, 043902 (2009)

X-ray scattering of polymer melts in uniaxial extensional flow

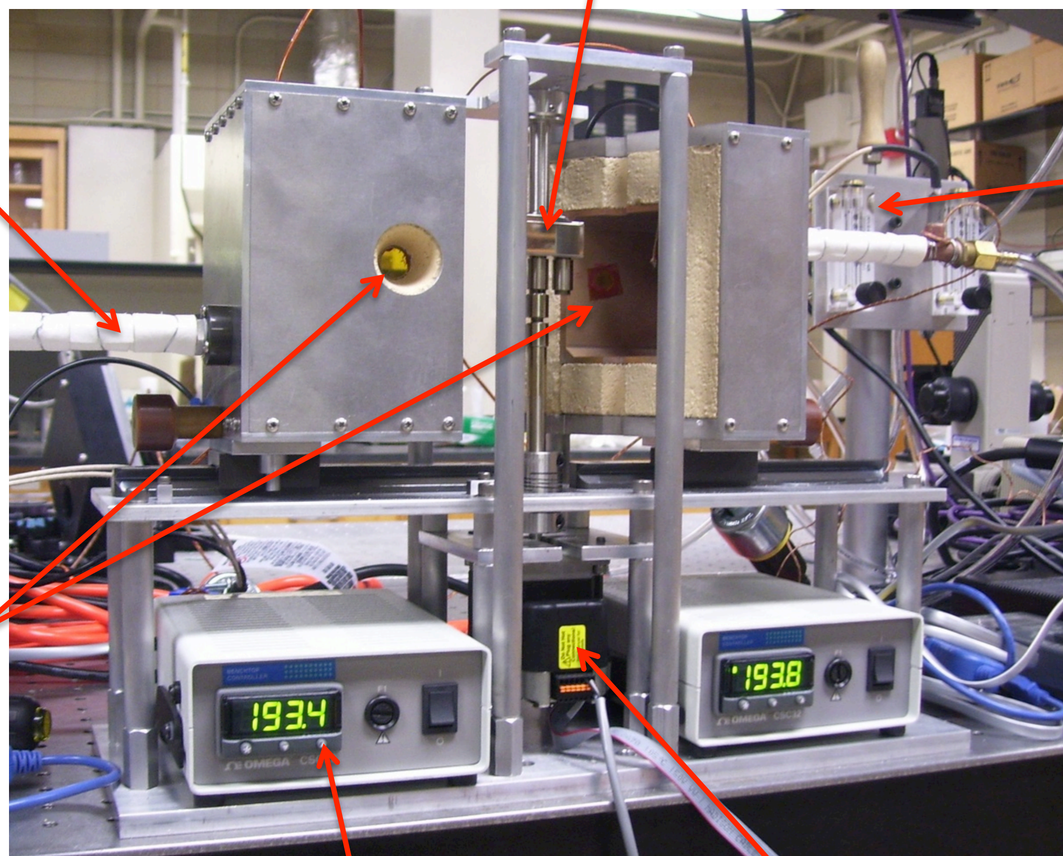

Summary

- X-ray scattering applied during flow & processing is a valuable tool
  - Insights into rheology; dynamics at microstructural level
  - Can access technologically relevant processing conditions
- Synchrotrons greatly facilitate such research
  - High flux: real-time data acquisition
  - High energy: facilitates design of rheo-x-ray instrumentation